1-1-2006

Accurate Method To Measure Harmonics And Interharmonics In Shipboard Power Quality Analysis

Anil Kumar Kondabathini

ACCURATE METHOD TO MEASURE HARMONICS AND INTERHARMONICS IN SHIPBOARD POWER QUALITY ANALYSIS

By

Anil Kumar Kondabathini

A Thesis
Submitted to the Faculty of
Mississippi State University
in Partial Fulfillment of the Requirements
for the Degree of Master of Science
in Electrical Engineering
in the Department of Electrical and Computer Engineering

Mississippi State, Mississippi

May 2006

ACCURATE METHOD TO MEASURE HARMONICS AND INTERHORMONICS IN SHIPBOARD POWER QUALITY ANALYSIS

By

Anil Kumar Kondabathini

Approved:

Dr. Herbert L. Ginn III Assistant Professor of Electrical and Computer Engineering (Major Advisor & Director of Thesis)	Dr. Michael Mazzola Professor of Electrical and Computer Engineering (Committee Member)
Dr. Randolph Follett Assistant Professor of Electrical and Computer Engineering (Committee Member)	Dr. Nicholas H. Younan Professor of Electrical and Computer Engineering (Graduate Coordinator)

Dr. Roger L. King
Associate Dean of College of Engineering

Name: Anil Kumar Kondabathini

Date of Degree: May 13, 2006

Institution: Mississippi State University

Major Field: Electrical and Computer Engineering

Major Professor: Dr. Herbert L. Ginn III

Title of Study: ACCURATE METHOD TO MEASURE HARMONICS AND INTERHARMONICS IN SHIPBOARD POWER QUALITY ANALYSIS.

Pages in Study: 65

Candidate for Degree of Master of Science

This thesis describes a novel approach that utilizes a special property of the Hanning window to accurately detect the fundamental frequency of the data signal in the presence of harmonic and interharmonic interference. After obtaining the fundamental frequency, the same procedure is applied to all possible harmonics to be filtered for further analysis of the interharmonics. The proposed approach is validated using numerical tests. In the literature, different authors have shown the difficulty of extracting a synchronized sampling frequency from the analyzed signal and discussed the effect of deviation of the fundamental in the presence of harmonics. This thesis suggests a new approach to overcome the difficulties, even if the interharmonics present are in frequency bins near the fundamental.

In order to perform the interharmonic analysis, the author followed the IEC standard draft signal processing recommendations, with the exception of using a weighted Hanning window instead of a rectangular window in order to minimize the

effect of the spectral leakage, and to minimize the effect of interharmonics on the main harmonics.

DEDICATION

I would like to dedicate this work to my family members.

ACKNOWLEDGMENTS

I would like to take this opportunity to express my deepest gratitude to my advisor Dr. Herbert L. Ginn III for his support, guidance, and encouragement throughout this research. I would also like to extend thanks to the other committee members Dr. Michael Mazzola, and Dr. Randolph Follett for serving on my committee to improve this work.

I would like to thank US Navy-Office of Naval Research (ONR) for financial support for this project.

I would also like to thank my parents, my brother and my friends for their support through out my academic career with out which I would not have dreamt about my M.S degree.

I would also like to thank my colleague Shane Cravens for his technical assistance in this work.

TABLE OF CONTENTS

CHAPTER Page

LIST OF TABLES

LIST OF FIGURES

FIGURE Page

FIGURE Page

CHAPTER I

INTRODUCTION

1.1 Introduction

Power Quality studies are gaining increased interest in order to analyze the impact of Power Electronic converters on Power System Equipment. Such converters are increasing in number and result in harmonic and interharmonic distortion. Parameter estimation of the harmonic components is very important for control and protection tasks. Also the design of harmonics filters relies on the measurement of distortions in both current and voltage waveforms. Some loads (adjustable-speed motor drives, welders, arc furnaces, static frequency converters, cyclo-converters etc.) also introduce changes in waveform periodicity because they are not pulsating synchronously with the fundamental power system frequency. This further complicates the power quality analysis. Relevant analysis can be processed by various signal-processing techniques related to the change of waveform periodicity.

Recent studies of power systems [1] revealed that even a small amount of interharmonics might cause serious problems with the lifetime of some power system equipment. According to these studies, severe vibration problems can be caused by resonance between the lowest mechanical natural frequency of a turbine-generator and the lowest interharmonic frequency from the electric power system, and this vibration can

grow to an unacceptable level resulting in a shutdown of the system. These resonance phenomena can be interpreted as a result of power transfer from the electrical interharmonic component to a relatively lightly damped mechanical resonance.

1.2 Objective of the research

Future naval electric distribution systems will contain an integrated electric drive system as well as be required to supply other demanding loads such as high power pulsed loads. Thus, this type of system will contain numerous high power nonlinear loads. The propulsion system in particular will be a type of adjustable speed motor drive, and therefore, will generate both harmonics and interharmonics. Power quality analysis of these systems will be more challenging than that of terrestrial systems due to higher variability of the fundamental frequency as well as interharmonic content. This thesis explores a technique that maintains a desired level of accuracy when performing power quality analysis under such difficult conditions.

1.3 Overview of Thesis

For the analysis of the interharmonics, the harmonic frequency components first have to be identified and then subtracted from the original data. To extract harmonics accurately it is important to find the fundamental frequency of the data to be analyzed. In previous papers [2]-[4] the authors have shown the difficulty of extracting a synchronized sampling frequency from the analyzed signal and discussed the effect of the deviation of the fundamental in the presence of the interharmonics. This thesis suggests a novel

approach to overcome the difficulties even if the interharmonics are present in a frequency spectrum near the fundamental.

The method discussed in this thesis follows the IEC standard draft [6] signal processing recommendations with the exception of using a weighted Hanning window instead of a rectangular window in order to minimize the effect of the spectral leakage, and to minimize the effect of the interharmonics on the main harmonics. To analyze the interharmonics, a signal processing technique called "Double Stage Harmonic and Interharmonic Processing Technique" [5] is used. Moreover, a new algorithm (based on Hanning window properties) is used to find harmonic frequencies instead of an interpolation procedure. This algorithm makes use of a weighted Hanning window for both stages, which is applied for all harmonics including the fundamental. Thus, error caused by negotiating the negative frequency replica is reduced, results in increased accuracy [7]. The use of the algorithm presented here involves tedious calculations, which can be ignored with the advent of modern computational software and high-speed digital computers.

The methods outlined in this thesis are validated using the data obtained from a case study performed aboard the USCGC Healy. The Healy contains a cyclo-converter drive system and presents an environment that is challenging with respect to a power quality study.

1.4 Thesis Organization

The contents of this thesis are summarized as follows. Chapter II discusses basic knowledge of the Naval Electric Shipboard Power System. It introduces the main differences between the Naval and terrestrial power distribution systems, then gives the general overview of various shipboard drive systems and the format of the output harmonics for the different types of drives.

Chapter III gives background information about the signal processing techniques for spectrum estimation and presents the synchronized and desynchronized-sampling concepts for a discrete sampled data signal.

Chapter IV discusses the processing of harmonic and interharmonic frequencies using a Hanning window and explains the effect of spectral leakage in the presence of desynchronization on the frequency spectrum. The later part of the chapter presents the special property of Hanning window based on which a novel algorithm is developed to find the fundamental frequency of the signal spectrum in the presence of desynchronization.

Chapter V and Chapter VI deal with the application of the proposed algorithm and its validation by analyzing numerical case study data, and then data from the USCGC Healy acquired during a power quality study, conducted by Northrop Grumman ship systems and Mississippi State University (MSU).

Chapter VII presents conclusions and suggestions for future work based on the proposed techniques.

CHAPTER II

NAVAL ELECTRICAL POWER SYSTEM

2.1 Introduction

The main difference between naval and land-based electrical power systems is the fact that a naval power system is an isolated system with short distances from the generated power to the load. The amount of installed power in vessels [8] may be high and this involves a special engineering challenge for such systems. The interconnections of the diverse systems on a vessel are increasingly complex, making the design, engineering and building of a vessel a more integrated effort. Figure 2.1 shows the single line diagram for a ship with podded electric propulsion.

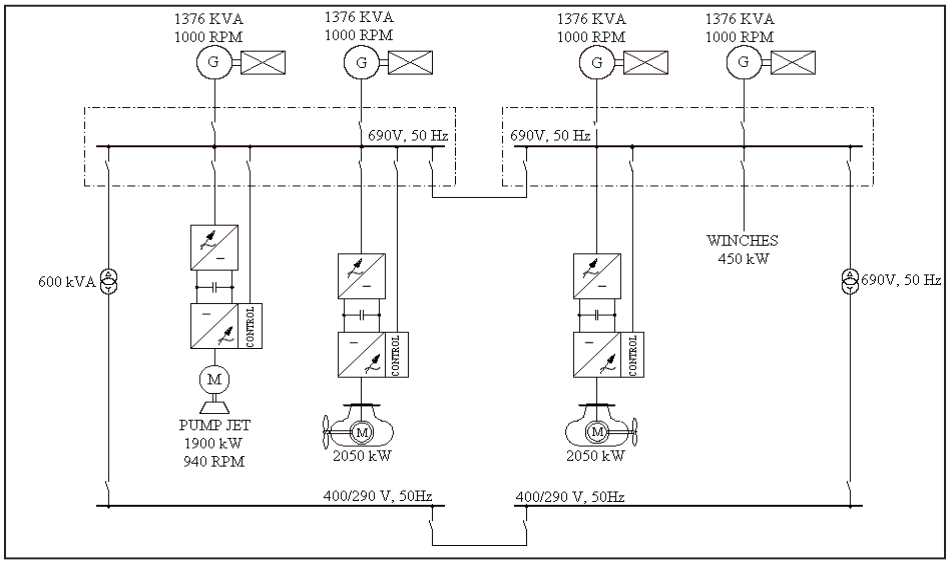

Figure 2.1 Single line diagram for a ship with podded electric propulsion. (Ref [8] Figure 3.1).

2.2 Electrical Power Generation and Distribution

Commercial vessels have an AC power generation plant with a hybrid (both AC and DC) [8] distribution system depending on the power distribution architecture. Some of the characteristics of the (vessel's) ship power distribution system are given as follows:

1. Have no infinite bus.
2. Prime movers are faster than utility case.
3. Have large dynamic loads.
4. Have large number of nonlinear loads relative to the generator capacity.
5. Have a short distance between the generator and loads.

2.3 Motor Drive for Propulsion and Thrusters

The electrical motor is the most commonly used device for conversion from electrical to mechanical power and is used for electric propulsion, thrusters for propulsion or station keeping, and other on-board loads such as winches, pumps, fans, etc. Figure 2.2 gives a schematic overview of a commercial vessel, showing the main electrical and automation components including thrusters, propulsion and drives. Typically, 80-90% of the loads in ship installations will be electrical motors [12]. The direct-on-line (DOL) motor will rotate with a speed directly determined by the network frequency.

The most commonly used motor drives are:

- Voltage source inverter (VSI) type converters for AC motors.
- Current source inverter type (CSI) converters for AC motors, normally synchronous motors.
- Cyclo-converters (Cyclo) for AC motors, normally for synchronous motors.
- DC converters, or Silicon Controlled Rectifiers (SCR) for DC motors.

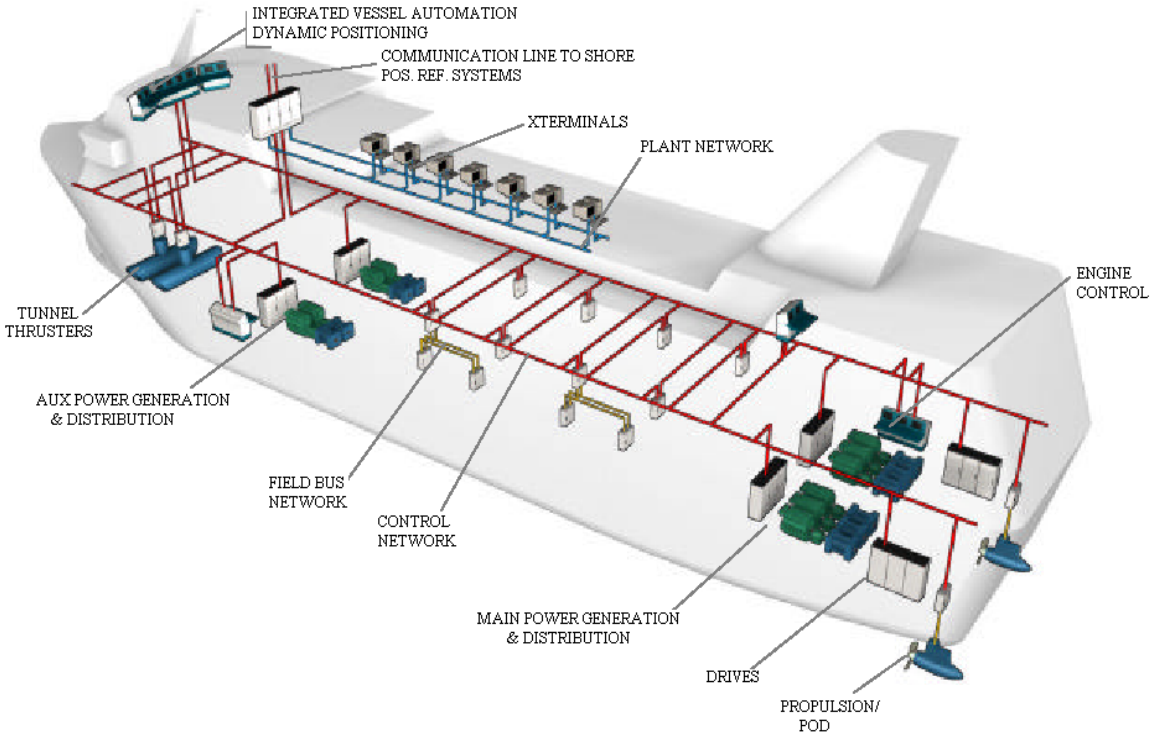

Figure 2.2 Schematic overview of the main electrical and automation components in a typical cruise vessel with diesel-electric podded propulsion (Ref [8] Figure 2).

In ships, most variable speed drives use AC motors. Most drives, except the cyclo-converters, will consist of a rectifier, which rectifies the line voltage, and an inverter, which generates the variable frequency and variable voltage source for motor.

A motor controller contains the speed control, and implements the control of motor currents by controlling the switching elements of the rectifier or inverter. An interface to an overriding control system, vessel management system, or dynamic position control is normally required. The motor controller acquires measurement signals and feedback signals from sensors in the drive, and motor. Figure 2.3 will depicts the motor speed control scheme [13]. Typically, motor currents, motor speeds, and voltages are measured. For practical reasons, the speed control loop of a motor drive can be regarded as a PI (or PID) controlled closed loop with an inner closed torque control loop, which for control purpose can be regarded as a first order time lag.

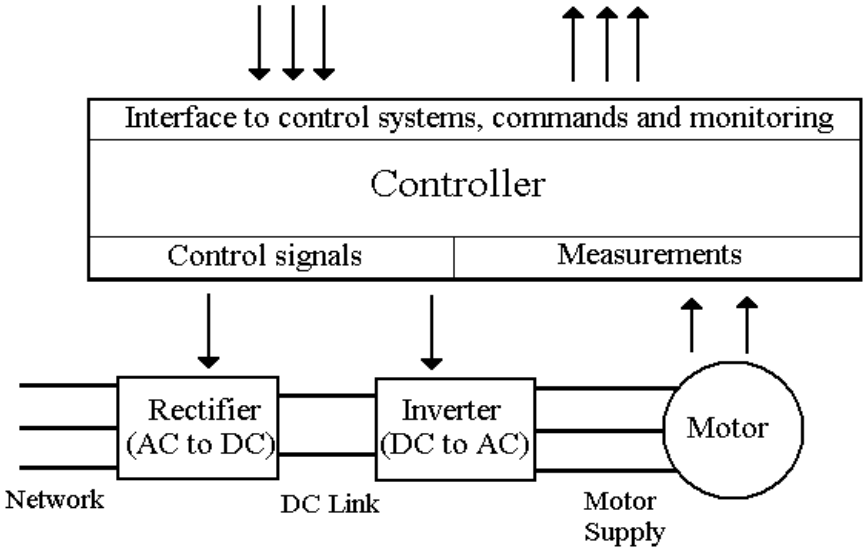

Figure 2.3 Schematic of a variable speed drive, showing a frequency converter with DC Link.

2.4 Cyclo-converters

The cyclo-converters (Cyclo) are direct converters without a DC link. The AC voltage is constructed by selecting phase segments of the supply voltage by controlling the anti-parallel thyristor bridge [14]. A 12-pulse configuration with reduced line

harmonics is shown in Figure 2.4, but the cyclo-converter can also be supplied in a 6-pulse configuration. In a 6-pulse configuration, the feeding transformers can be substituted with reactors when the supply voltage matches the inverter voltage.

The cyclo-converter has been preferred in applications where low speed operation and performance is essential, especially in ice breaking or ice going systems, but also in passenger vessel applications where low speed performance is essential.

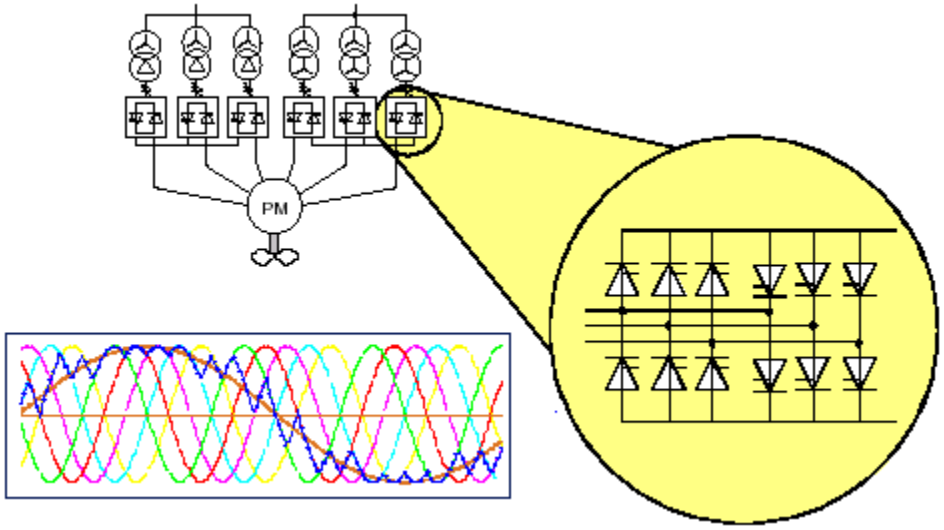

Figure 2.4 Cyclo-converter drives with input and fundamental output waveforms. The output voltage is constructed by selecting phase segments of the supply voltage. (Ref [8] Figure 5.4).

2.4.1 Output and Input Harmonics

The cyclo-converter output voltage waveform has complex harmonics. Higher order harmonics are usually filtered by the machine inductance; therefore the machine current has fewer harmonics. The remaining harmonics, cause harmonic losses and torque pulsations.

There are several factors affecting the harmonic content of the waveforms. The blocking mode of operation produces more complex harmonics than the circulating mode of operation due to the zero current distortion. In addition to this, the pulse number affects the harmonic content. A greater number of pulses have less harmonic content. Therefore, a 6-pulse (bridge) cyclo-converter produces fewer harmonics than a 3-phase (half-wave) cyclo-converter. Moreover, as the output frequency gets closer to the input frequency, the harmonics increase. Finally, low power factor and discontinuous conduction both contribute to harmonics.

For a typical p-pulse converter, the order of the input harmonics is "$pn \pm 1$" and that of the output harmonics is "pn", where 'p' is the pulse number and 'n' is an integer. Thus for a 3-pulse converter the input harmonics are at frequencies $2f_i$, $4f_i$ for n=1, $5f_i$, $7f_i$ for n=2, and so on. The output harmonics, on the other hand, are at frequencies $3f_i$, $6f_i$, …

2.5 USCGC Healy Power System

The proposed technique has been studied by its application to data acquired from USCGC Healy. Electrical data has been acquired on a voyage aboard the USCGC Healy by way of the Northwest Passage during the summer of 2003. The electrical data has been acquired at multiple locations on the ship under various operating conditions. Operating parameters of the ship during the data acquisition included numerous conditions such as a bollard, in which the ship pushed against an immovable piece of ice with a significant thrust, a crash - reversal in which the ship was brought to a stop by reversing its motors, and finally several controlled ramps in speed. Data recorded during

these various scenarios has enabled evaluation of the impact of the drive system under its full range of operation.

The Healy contains two 12-pulse cyclo-converter drive systems supplied from four 7.2MW generators as shown in the one-line diagram in Figure 2.5. Power quality analysis of such a system is more challenging than that of terrestrial systems, due to higher variability of the fundamental frequency as well as high interharmonic content.

Real-time waveform voltage and current data was acquired at a sampling frequency of 7680Hz at multiple locations in the distribution system. Data was acquired on the medium voltage bus (6600 V) and on both the ship non-sensitive bus and the ship sensitive bus for the low voltage (450 V) network. A National Instruments PXI Data Acquisition unit with two PXI-6052E DAQ devices was used in order to acquire 16 channels simultaneously. The device was configured for remote operation via the ships fiber network. This enabled more precise coordination with the other data acquisition equipment located throughout the ship.

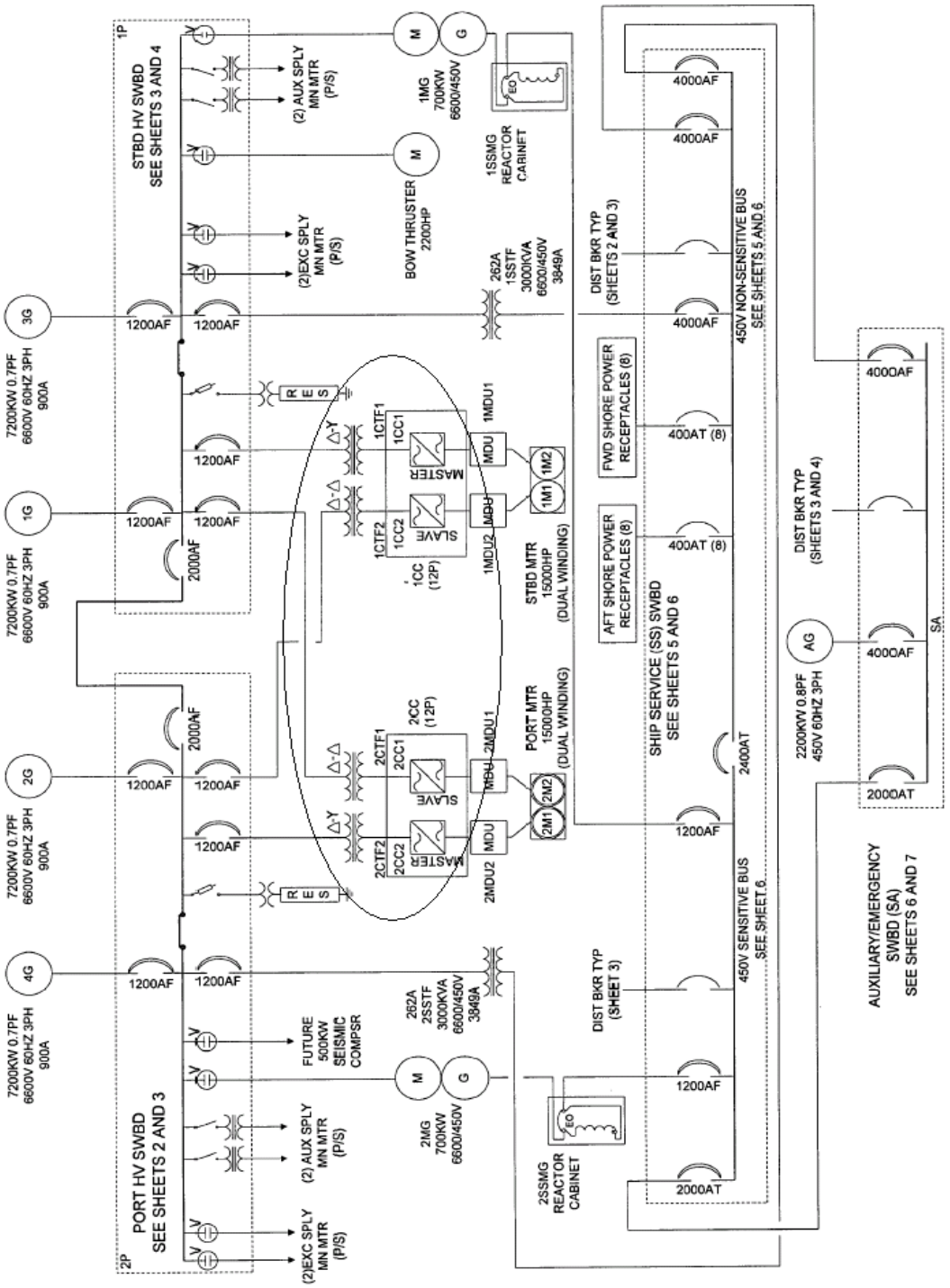

Figure 2.5. USCGC Healy Cyclo-converter Drive System. (Ref [16] Figure 8)

CHAPTER III

DIGITAL SIGNAL PROCESSING BACKGROUND

3.1 Introduction

This chapter will introduce some of the basic signal processing techniques to understand the concepts of windowing, spectrum estimation, and frequency spectral leakage in sinusoidal signal estimation.

3.2 Discrete Fourier Transform

The Discrete-Time Fourier Transform (DTFT) of a sequence is a continuous function of that sequence, and repeats with period 2π. In practice, the Fourier components are obtained using digital computation and can only be evaluated for a discrete set of frequencies. The discrete Fourier transform (DFT) provides a means for achieving this [10].

The DFT is itself a sequence, and it corresponds roughly to samples, equally spaced in frequency, of the Fourier transform of the signal. The discrete Fourier transform of a signal $x[n]$, with a sample length N is given by,

$$X[k] = \sum_{n=0}^{N-1} x[n] e^{-j(2\pi/N)kn} . \tag{3.1}$$

The corresponding equation for the inverse DFT is given by,

$$x[n] = \frac{1}{N}\sum_{k=0}^{N-1} X[k]e^{j(2\pi/N)kn} . \tag{3.2}$$

When expressing the DFT, it is common to define the complex quantity

$$W_N = e^{-j(2\pi/N)} . \tag{3.3}$$

By substituting this notation in the DFT pair of Equation (3.1) and Equation (3.2), the pair becomes:

$$X[k] = \sum_{n=0}^{N-1} x[n]W_N^{kn} \tag{3.4}$$

$$x[n] = \frac{1}{N}\sum_{k=0}^{N-1} X[k]W_N^{-kn} . \tag{3.5}$$

3.3 Spectrum Estimation

Spectrum estimation is the task of estimating the DTFT of a signal $x[n]$. The DTFT of a discrete-time signal $x[n]$ is

$$X(e^{j\omega}) = \sum_{n=-\infty}^{\infty} x[n]e^{-j\omega n} . \tag{3.6}$$

The signal $x[n]$ is generally of infinite duration in theory, and $X(e^{j\omega})$ is a continuous function of ω. The DTFT can therefore not be calculated using a computer.

Consider that we truncate the signal $x[n]$ by multiplying with the rectangular window $w_r[n]$ or a Hanning window $w_h[n]$. For a rectangular window, the windowed signal is $X_w[n] = x[n]w_r[n]$, and the DFT is given by,

$$X_w(e^{j\omega}) = \sum_{n=-\infty}^{\infty} x_w[n]e^{-j\omega n} = \sum_{n=0}^{N-1} x_w[n]e^{-j\omega n} . \tag{3.7}$$

Noting that the DFT of $x_w[n]$ is

$$X_w[k] = \sum_{n=0}^{N-1} x_w[n] W_N^{-kn}, \tag{3.8}$$

this equation can be rewritten as

$$X_w[k] = X_w(e^{j\omega})\big|_{\omega=2\pi k/N}, \tag{3.9}$$

i.e., the values of the DFT $X_w[k]$ of the signal $x_w[n]$ are therefore periodic samples of the DTFT $X_w(e^{j\omega})$, where the spacing between the samples is $2\pi/N$. Since the relationship between the discrete-time frequency variable and the continuous-time frequency variable is $\omega = \Omega T$, the DFT frequencies corresponds to continuous-time frequencies

$$\Omega_k = 2\pi k / NT. \tag{3.10}$$

The DFT can therefore only be used to find the points on the DTFT of the windowed signal $x_w[n]$ of $x[n]$. For a simple rectangular window, the frequency response is shown in Figure 3.1:

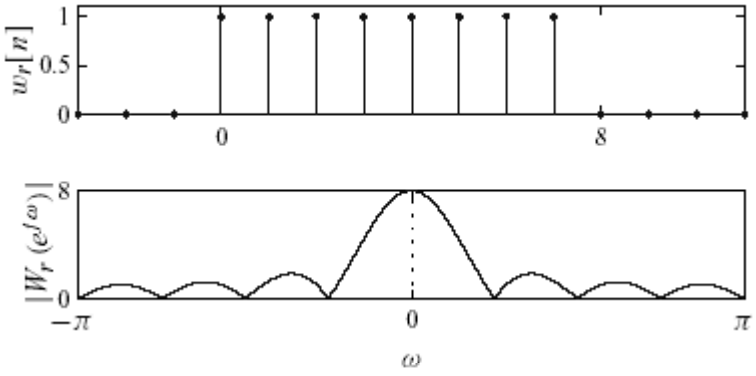

Figure 3.1 Continuous frequency response of a rectangular window.

where

$$W_r(e^{j\omega}) = \frac{\sin(\omega N/2)}{\sin(\omega/2)} e^{-j\omega(N-1)/2}. \tag{3.11}$$

3.4 Spectrum analysis of Typical Sinusoidal Signals

Suppose we have a sinusoidal combination

$$x[n] = \cos(\pi/3n) + 0.75\cos(2\pi/3n), \qquad -\infty < n < \infty. \tag{3.12}$$

Since the signal is infinite in duration, the DTFT cannot be computed numerically using a digital computer. Therefore the signal is windowed in order to make the duration finite as shown in Figure 3.2:

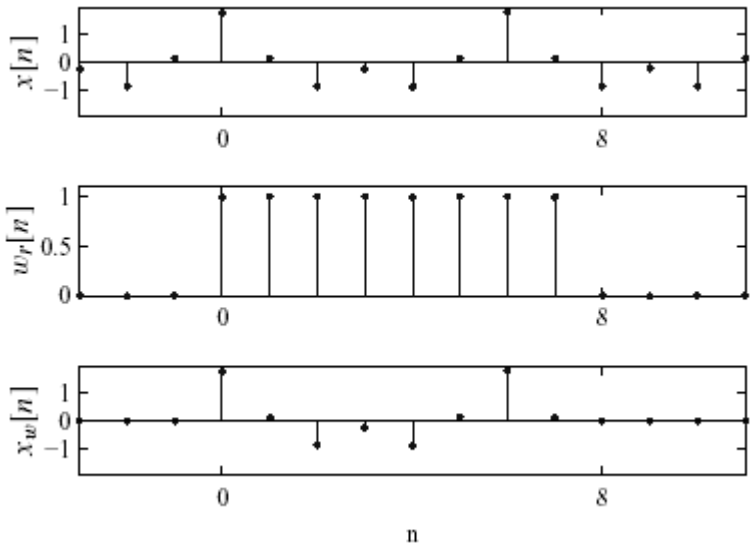

Figure 3.2 Weighting signal with rectangular window to make it finite.

The operation of the windowing modifies the signal. This is reflected in the discrete-time Fourier transform domain by a spreading of the frequency components shown in Figure 3.3:

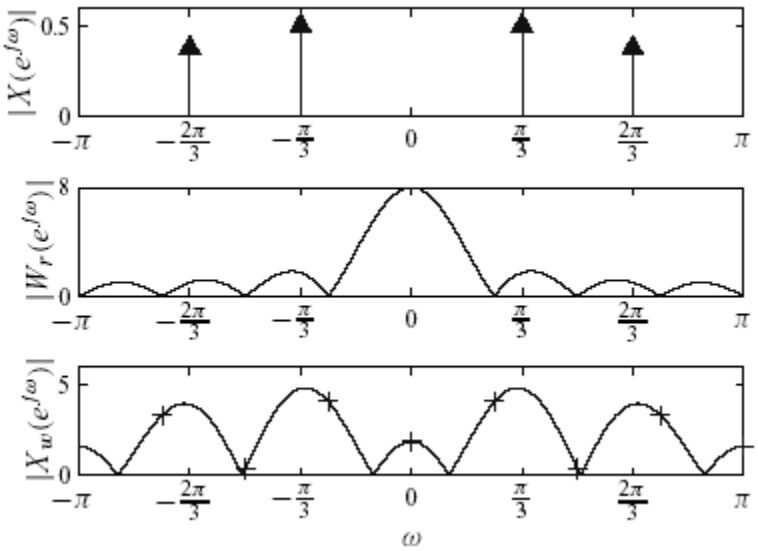

Figure 3.3 Frequency components in DTFT domain after windowing.

The operation of windowing therefore limits the ability of the Fourier transform to resolve the closely spaced frequency components. When the DFT is used for spectrum estimation, it effectively samples the spectrum of this modified signal at the locations of the crosses indicated in Figure 3.3 and resulted frequency spectrum is shown in Figure 3.4:

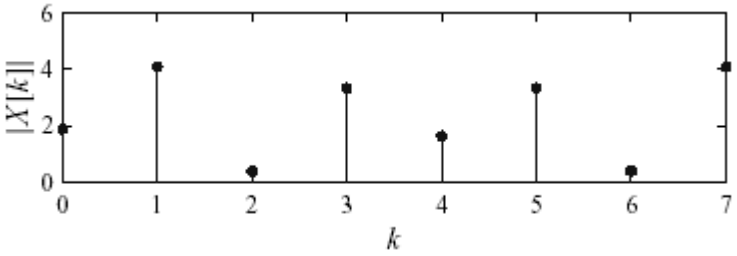

Figure 3.4 Frequency spectrum of the signal from Equation 3.12.

here, $k = 0$ corresponds to $\omega = 0$ in the discrete domain. In general, the elements of the N-point DFT of $x_w[n]$ contain N evenly spaced samples from the DTFT $X_w(e^{j\omega})$. It is also possible to get more samples with a closer spacing by performing more computation.

As the length N of the data window increases, the windowed signal $x_w[n]$ becomes a better approximation of $X_w(e^{j\omega})$.

In general the rectangular windowing process causes two major effects on the frequency spectrum:

1. It reduces the frequency resolution of the computed spectrum.
2. It introduces an effect called "*frequency spectral leakage",* which is caused by the sharp clipping of the signal x [n] at the left and right ends of the rectangular window [9].

The results give less error if we deal with the Hanning window, for which the windowed signal is $X_w[n] = x[n]w_h[n]$. Using the Hanning window, the windowed data at the boundaries are smoothly brought to near zero [9].

The Hanning window is given by,

$$w_h[n] = \begin{cases} 0.5\left(1 - \cos\left(2\pi \frac{n}{N}\right)\right) & \text{if } 1 \le n \le N \\ 0, & \text{otherwise} \end{cases} \tag{3.13}$$

and the frequency function is given by [9]

$$W_h(e^{j\omega}) = 0.5D(\omega) + 0.25\left(D(\omega - \frac{2\pi}{N}) + D(\omega + \frac{2\pi}{N})\right), \tag{3.14}$$

where

$$D(\omega) = \frac{\sin(\omega N/2)}{\sin(\omega/2)} e^{j\omega/2} \tag{3.15}$$

Figure 3.5 shows the points on the DTFT of a simple Hanning windowed signal $w_h[n]$ of $x[n]$.

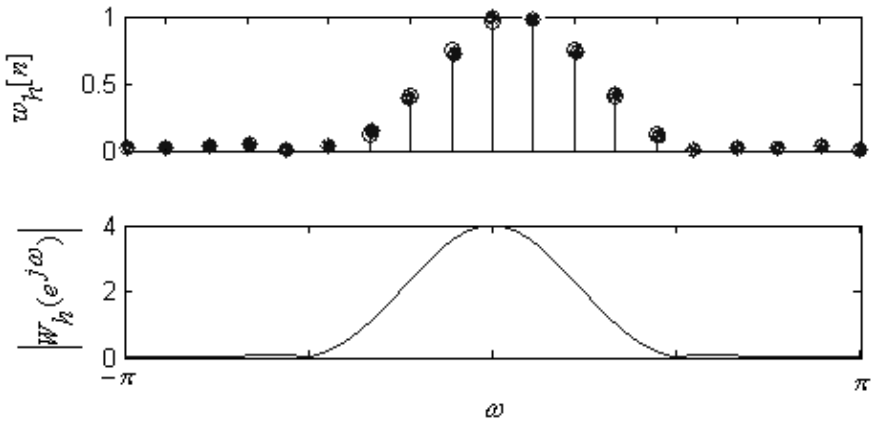

Figure 3.5 Frequency response of a Hanning window.

It can be noted from Figure 3.5 that when compared with the rectangular window Figure 3.1, the frequency spectrum data at the boundaries are smoothly brought to near zero, thus reducing the frequency spectral leakages.

CHAPTER IV

PROCESSING OF HARMONICS AND INTERHARMONICS USING HANNING WINDOW

4.1 Introduction

Harmonics are spectral components at the frequencies that are integer multiples of the fundamental frequency. The interharmonics are spectral components at frequencies that are not integer multiples of the fundamental frequency.

IEC-61000-2-1 defines interharmonics as:

"*Between the harmonics of the power frequency voltage and current, further frequencies can observed which are not integer multiples of the fundamental. They can appear as discrete frequencies or as a wide-band spectrum*".

Usually, in real-time data, the content of the interharmonics is more at increasing loads for non-linear devices. Presence of these devices produces periodic but non-sinusoidal voltages and currents called interharmonics. They create additional problems like light flickering and voltage fluctuations in the system. Due to the presence of the harmonics, we have more than one sinusoidal signal along with the interharmonics. We are primarily interested in interharmonics. To analyze the content of the interharmonics it will be sensible, if we remove the fundamental and its harmonics as perfectly as possible

from the sampled signal, since the remaining part consists of the interharmonics that we want to analyze.

To process the interharmonics the basic approach is:

1. Find the fundamental frequency of the data to be analyzed.
2. Determine the harmonics from the spectral component.
3. Remove the harmonics from the spectrum.
4. Analyze the rest of the spectrum for interharmonics.

4.2 Determination of the Harmonics

While dealing with real-time data we need to overcome two factors in order to precisely analyze its harmonic content from the spectrum

1) Spectral Leakage
2) Desynchronization

If we can determine the fundamental frequency by overcoming the above two factors, then we can easily find its harmonic content.

To overcome this, we used a popular technique in signal processing called the *interpolation FFT method* [7] with a Hanning window. The use of a Hanning window will reduce the spectral leakage considerably, and the *interpolation technique* will help in determining the fundamental frequency component along with its amplitude and phase.

4.2.1 Effect of Desynchronization

Let us discuss the effect of spectral leakage in the presence of desynchronization on frequency spectrum. The desynchronization is due to incoherent sampling. This is

explained using a test sampling. An integer number of cycles of the fundamental period needs to be used, with fundamental frequency

$$f_i = \frac{T_W}{N} f_s , \tag{4.1}$$

where f_i is the actual value of fundamental frequency, T_W is an integer equal to the number of cycles of the fundamental time period (width of the window in terms of number of cycles), N is the number of samples in the record, and f_s is the sampling frequency. But in practice, the value of f_s may not be an exact integer multiple of the fundamental, resulting in incoherent sampling or desynchronization.

To explain desynchronization, it is better to consider a typical DFT result calculated from incoherently sampled data, as shown in Figure 4.1.

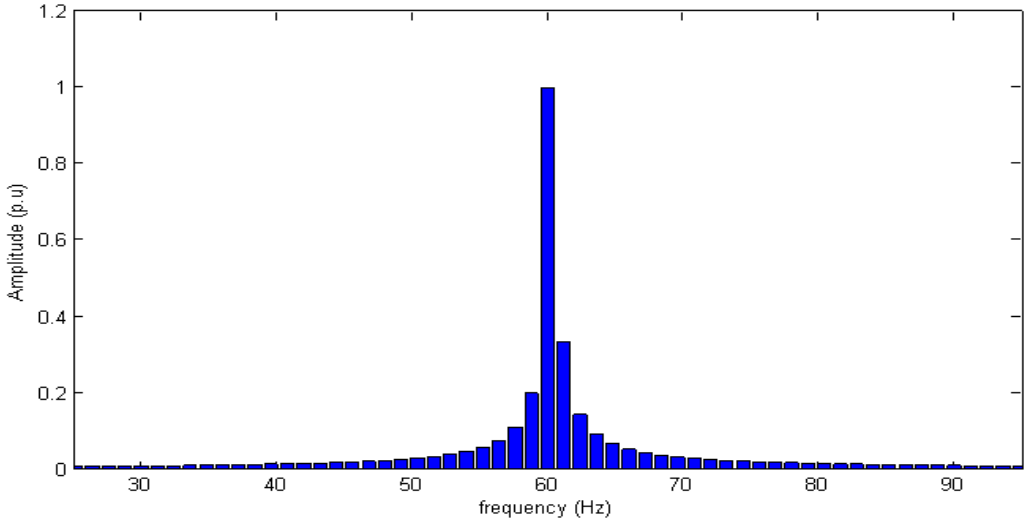

Figure 4.1 Typical DFT using a rectangular window of an incoherently sampled sine wave, f_i = 60.3Hz.

The incoherently sampled data is derived from the following continuous spectrum (Figure 4.2) of rectangular windowed waveform. Here, the marked lines corresponding to

the frequency spectrum of an incoherently sampled sine wave. Figure 4.2 shows the individual frequency bins of the window function positioned around the fundamental frequency of the sine wave. The exact frequency of the sine wave should be between the adjacent large peaks.

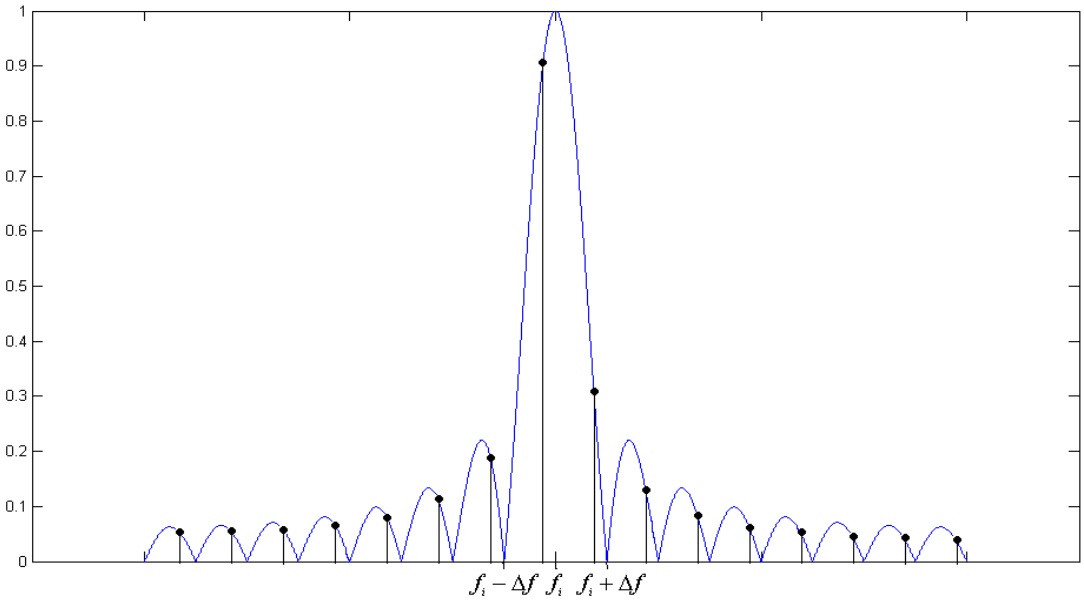

Figure 4.2 Rectangular window of an incoherently sampled sine wave, $f_i = 60.3$Hz.

The true frequency of the sine wave is at most $\Delta f / 2$ from the place of the maximum peak, and the value of the maximum amplitude is also down from the theoretical value and is distributed among all individual bins. Here, the value of Δf is given by

$$\Delta f = \frac{f_s}{N} \tag{4.2}$$

Thus, the desynchronization will introduce inaccuracy for determining the frequency component of the sine function. This inaccuracy is too much for our analysis purpose; especially due to the fact that the value of the amplitude and phase of the sine

component will vary from the true value. This will become more complicated in the presence of harmonics (other frequency sine wave components), because each incoherently sampled sine wave results in overlapping with components in adjacent frequency bins (spectral leakage). The cause of the leakage is due to the use of the rectangular window. The idea is then to modify the shape of the window function to have minimum side lobes.

4.2.2 Use of Hanning window to reduce the leakage

To reduce spectral leakage, we typically use a window function, such as a ``Hanning window'', to taper (reducing the side lobes) the data record gradually to zero at both endpoints of the window. As a result of the smooth tapering, the main lobe widens and the side lobes decrease in the DFT spectrum, resulting in fewer bins and reduced peak amplitude [9].

Figure 4.3 shows the improvement over the Rectangular window. Here, the true frequency of the sine wave is at most $\Delta f / 2$ from the place of the maximum peak. But this window function is more helpful in finding the fundamental frequency component in the presence of harmonics and interharmonics.

Figure 4.3 is derived from a continuous spectrum Hanning window, as shown in Figure 4.4, where the marked lines correspond to the frequency bins of an incoherently sampled sine wave.

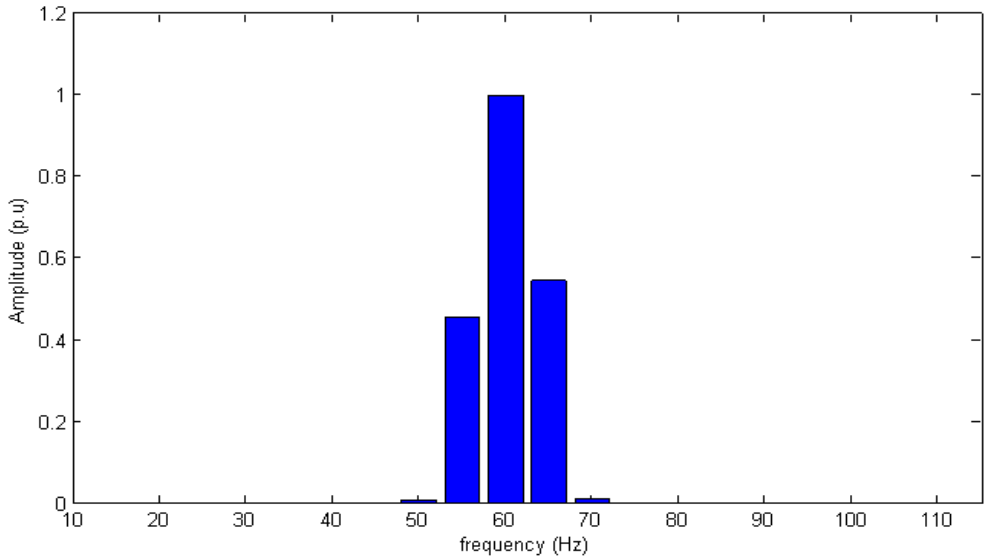

Figure 4.3 Typical DFT using a Hanning window on an incoherently sampled sine wave, $f_i = 60.3\text{Hz}$.

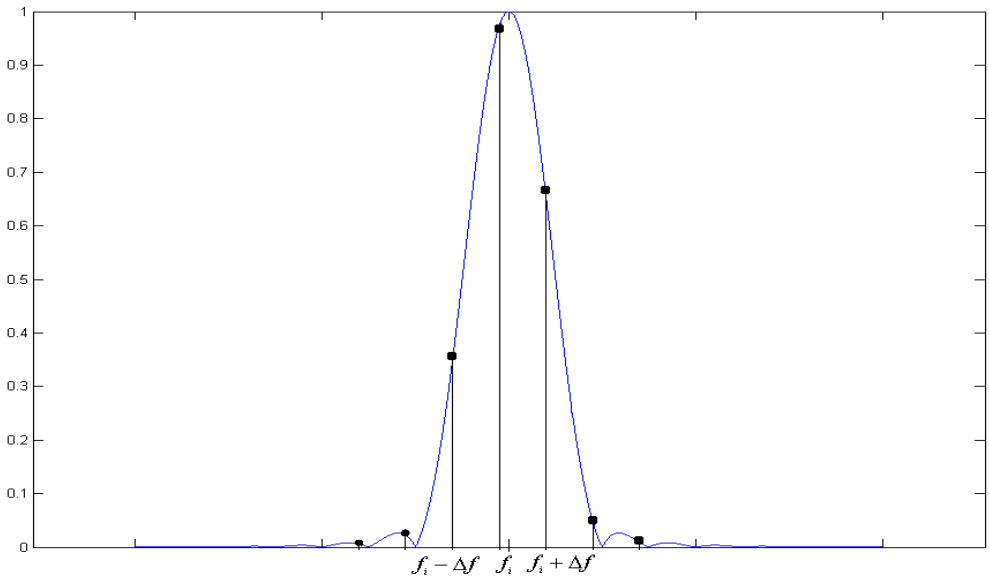

Figure 4.4 Hanning window of an incoherently sampled sine wave, $f_i = 60.3\text{Hz}$.

Now, consider a coherently sampled sine wave weighted with a Hanning window, where the value of the sampling frequency is an exact multiple of the fundamental frequency. Here, the maximum amplitude of the continuous Hanning window exactly

coincides with peak DFT spectral component of the Hanning window. This is shown in Figure 4.5.

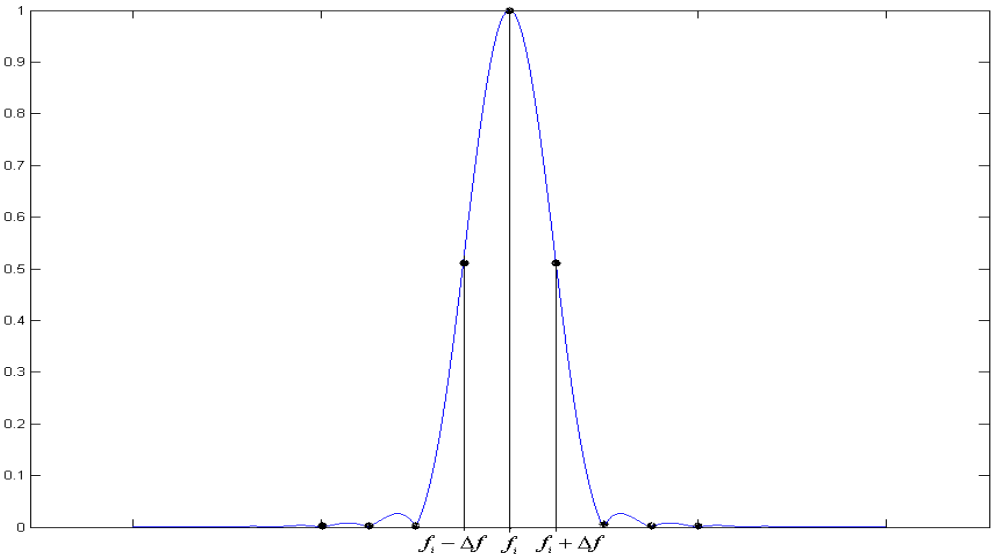

Figure 4.5 Hanning window of a coherently sampled sine wave, $f_i = 60$Hz.

The discrete spectrum is given in Figure 4.6. Thus the spectral leakage is decreased considerably when compared to that obtained when using a rectangular window.

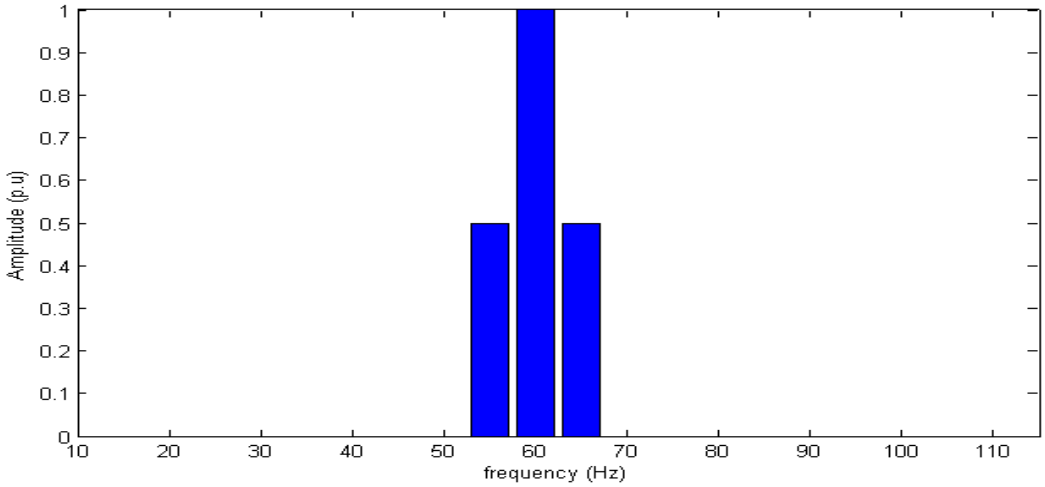

Figure 4.6 Typical DFT using Hanning window of an coherently sampled sine wave, f_i=60Hz.

The reduction in the spectral leakage will improve the accuracy in finding the value of the fundamental frequency, in the presence of harmonics and interharmonics. Once an accurate value of the fundamental frequency is obtained, we can find the harmonics and interharmonics with greater accuracy.

4.3 Special Property of Hanning Window

Now, consider only the main lobe of the continuous spectrum of a Hanning window, and elaborate on the previous discussion to better understand what exactly is happening when the signal is incoherently sampled.

As can be seen in Figure 4.7, with the presence of desynchronization between the actual frequency and sampled frequency, none of the DFT components matches the actual frequency f_i.

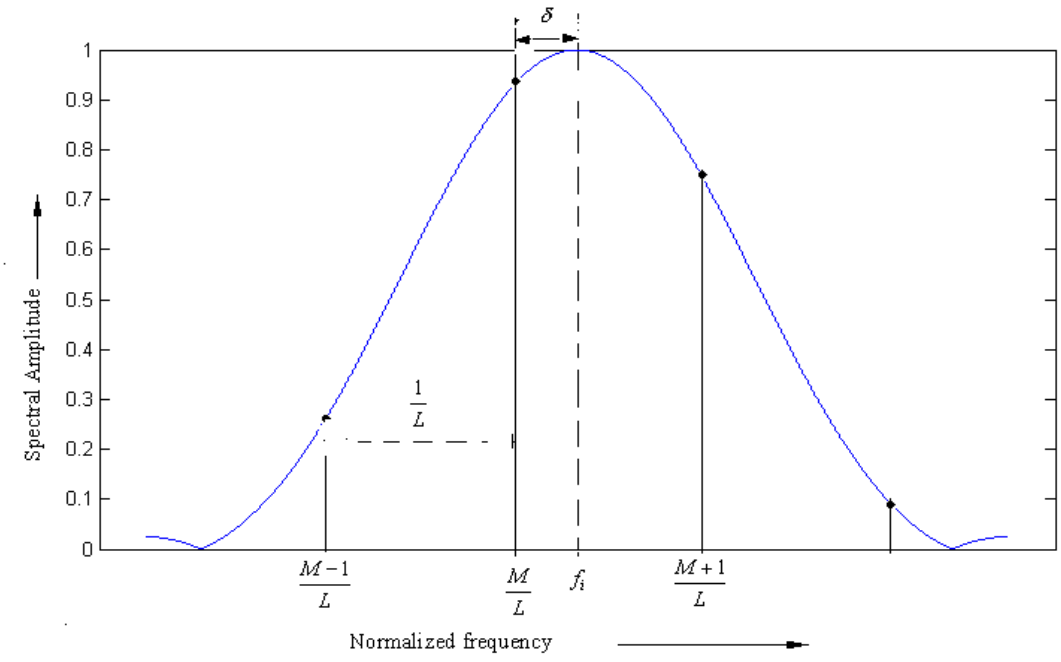

Figure 4.7 Main Lobe of the continuous spectrum of Hanning window.

From Figure 4.7, the actual frequency is given by,

$$f_i = \frac{M}{L} + \delta \tag{4.3}$$

where the value of M is the integer nearest to $f_i L$, and $\frac{1}{L}$ represents the normalized DFT frequency resolution, given by

$$L = \frac{N}{f_s} \tag{4.4}$$

and the value of the f_i is

$$f_i = (M + \delta)\frac{1}{L}, \qquad \text{in the range } \frac{M}{L} \le f_i \le \frac{M+1}{L}. \tag{4.5}$$

Let $\lambda = (M + \delta)$, and the Equation (4.5) becomes:

$$f_i = \lambda \frac{1}{L}. \tag{4.6}$$

So, the accuracy of the actual frequency of the given sine function is dependent on the accuracy of the shifted value δ. The value of δ is either positive or negative, depending on that particular situation, i.e. whether the window is shifted towards the left or towards the right. The sign is determined by

$$\delta \quad \text{is} \quad \begin{cases} \text{positive if} & S(M+1) \ge S(M-1) \\ \text{negative if} & S(M+1) \le S(M-1) \end{cases}, \tag{4.7}$$

where S is the DFT spectrum of the windowed signal [5], given by

$$S(i) = -0.5jA_1\left[e^{j(a(\lambda-i)+\phi_1)}\frac{\sin\pi(\lambda-i)}{\sin\pi(\lambda-i)/N} - e^{-j(a(\lambda+i)+\phi_1)}\frac{\sin\pi(\lambda+i)}{\sin\pi(\lambda+i)/N}\right], \tag{4.8}$$

In Equation (4.8), the value of i is given by $i = 0,1,2.....N-1$, for the input signal having only the fundamental frequency,

$$x_1(t) = A_1 \sin(2\pi f_1 t + \phi_1) \tag{4.9}$$

and for the multi-frequency signal

$$x\ (t) = \sum_{m=1}^{K} A_m \sin(2\pi f_m t + \phi_m) \tag{4.10}$$

The DFT spectrum for this multi-frequency signal [5] is given by

$$S(i) = -0.5j \sum_{m=1}^{K} A_m \left[e^{j(a(\lambda_m - i)+\phi_m)} \frac{\sin \pi(\lambda_m - i)}{\sin \pi(\lambda_m - i)/N} - e^{-j(a(\lambda_m + i)+\phi_m)} \frac{\sin \pi(\lambda_m + i)}{\sin \pi(\lambda_m + i)/N} \right] \tag{4.11}$$

where $a = \dfrac{\pi(N-1)}{N}$,

f_1 = Fundamental frequency,

A_1 = Amplitude of the fundamental frequency,

ϕ_1 = Phase of the fundamental frequency,

A_m, ϕ_m, f_m = Amplitudes, phases and frequencies of the harmonics.

The DFT does not give the exact value of δ, because it is not a continuous function and gives the values only for N samples of that particular case.

Thus, for a fundamental frequency of f_1 = 50, from direct DFT analysis, we will get the closest bin frequency either as 45, 50, or 55Hz for a desynchronized frequency. This can be overcome by means of interpolation of the spectrum samples calculated by DFT [7] [9].

One of the ways to improve the accuracy of δ is to use more sampled values for the weighted Hanning window, by taking a larger number of DFT values of continuous in the Hanning window.

This involves tedious calculations to find the value for each sample of window, but with the advent of modern computational software and high speed digital computers, all we need to develop a suitable cumulative algorithm and write the program to get as many sampled values as we can. So, there is trade-off between the accuracy of finding the fundamental frequency and the calculation burden.

4.4 Finding the Fundamental Frequency: Using Hanning window property

From the analysis of continuous frequency spectrum of Hanning window, the following property was observed:

In a continuous frequency spectrum of Hanning window, there exists a unique relation between 'δ' (desynchronization) and the difference in the '*Amplitudes of Rated Position Frequencies*' of either side of the position frequency of maximum amplitude of the spectrum, i.e. $S(M-1)$ and $S(M+1)$.

A simulation method is developed in this thesis to find this relation. From this relation, by finding the difference in the amplitudes of rated position frequencies, we can find the value of the δ, and thus the frequency corresponding to the respective desynchronization. Figure 4.8 shows the results of the simulation giving the relation between the difference in amplitudes of the rated position frequencies and the extent of the desynchronization.

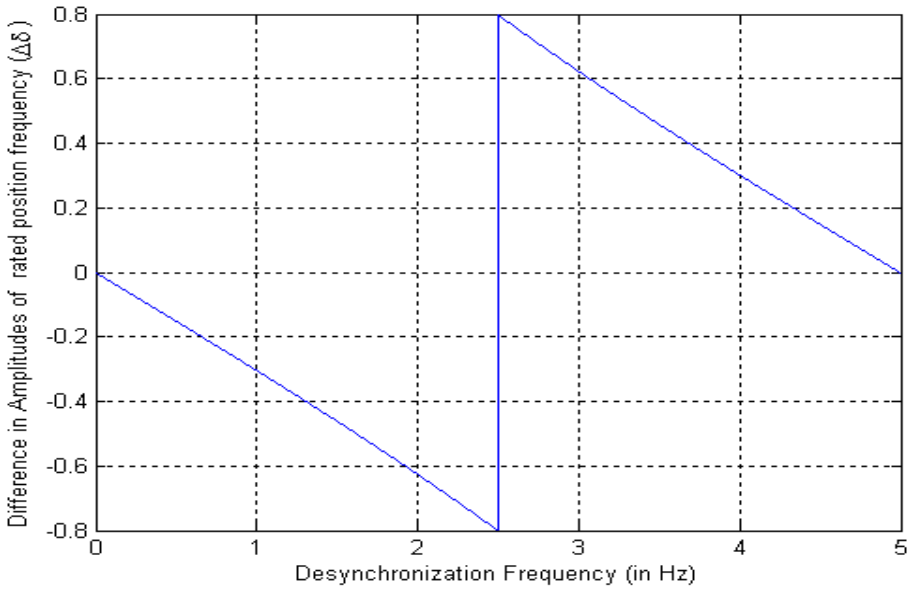

Figure 4.8 Difference in amplitudes of rated position frequency with the desynchronization.

To improve the accuracy of δ, a greater number of sampled values for the weighted Hanning window with the given fundamental frequency (f_i) are considered by taking a greater number of DFT values of the continuous Hanning window.

4.4.1 Algorithm

Here, an algorithm is developed for a 60Hz system and can be modified for the other systems accordingly. This algorithm is based on the unique relation of the value of δ with the rated position frequencies of either side of the position frequency of maximum amplitude of the spectrum as stated above.

This algorithm involves two sub-algorithms to find the value of δ. First, we get a template from the results of a known system, and then compare these results with the results from analysis of an unknown system.

Step. 1: Using the weighted Hanning window, and varying the fundamental frequency (f_i) from f_1 to $f_1 + \frac{1}{L}$, generate the template values of δ' for all possible values of difference in amplitudes of the rated position frequencies of either side of the position frequency of maximum amplitude of the spectrum. Figure 4.9 illustrates a flowchart of the procedure with the typical situation.

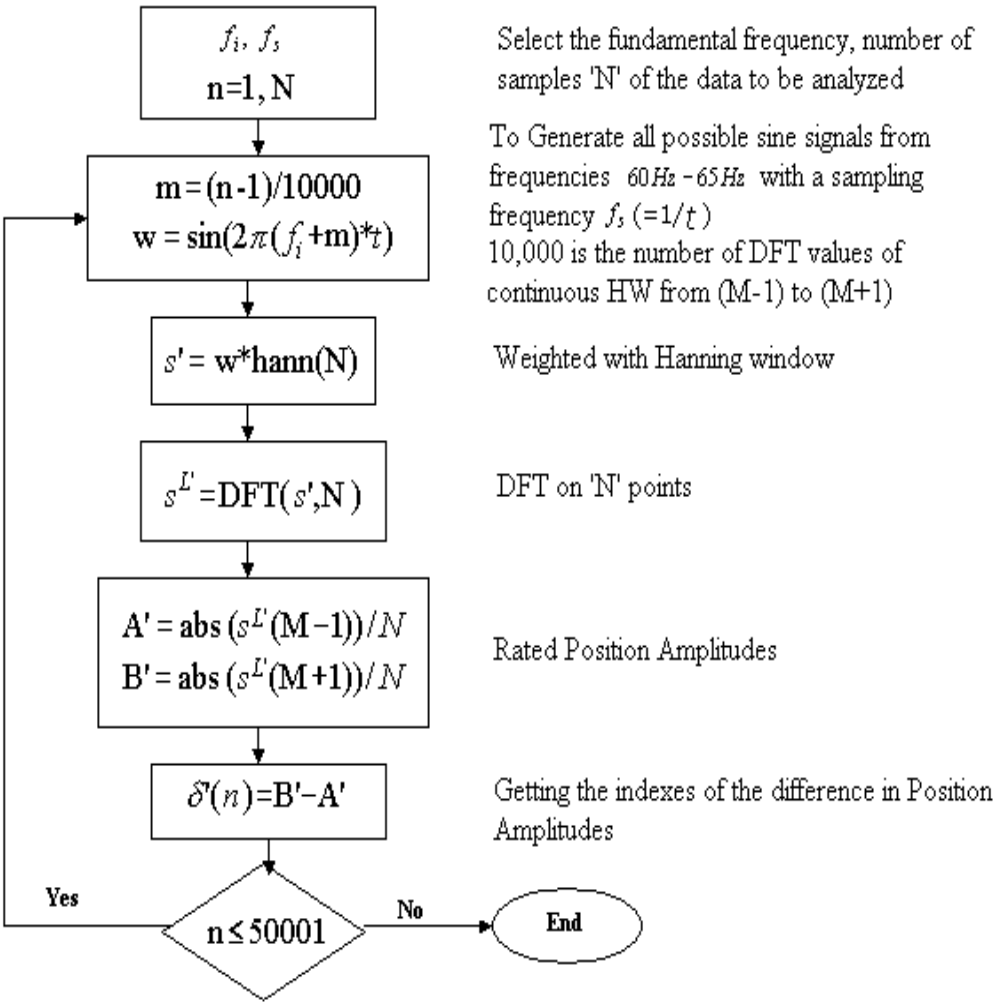

Figure 4.9 Describing the procedure through the Flow-Chart of the procedure for Step 1 of the Algorithm.

Step. 2: Find the value of the difference in the amplitudes of the rated positional frequencies, i.e., $S(M+1)$ and $S(M-1)$, for the given sampled input signal, and then compare this with the actual template values for δ' generated from the Step 1, in order to get the value of δ. Figure 4.10 illustrates a flowchart implementing the procedure for Step 2.

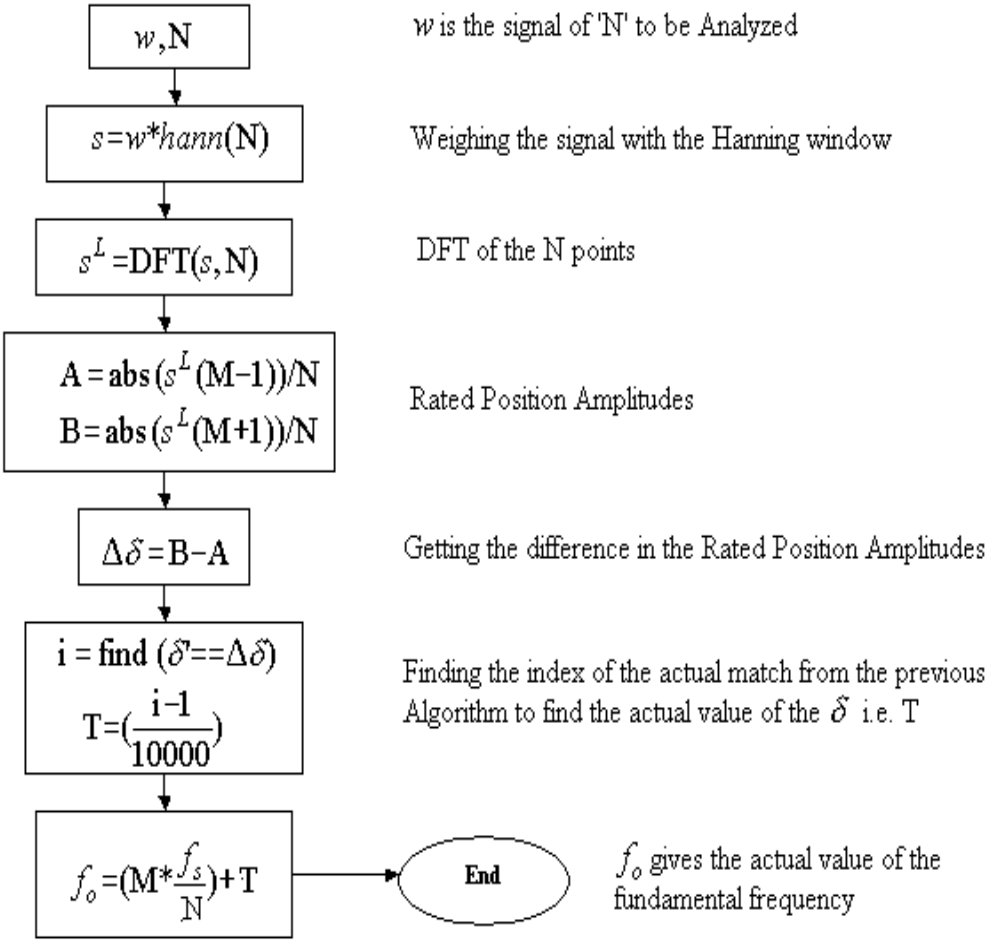

Figure 4.10 Describing the procedure through the Flow-Chart for Step 2 of the Algorithm.

This algorithm involves basic DFT calculations and windowing concepts, which were discussed earlier. The flowcharts shown in Figure 4.9 and Figure 4.10, illustrate the implementation of the procedure of Step 1 and Step 2 with reference to a 60Hz system. To obtain low sensitivity to the spectrum leakage effects during the analysis stage, it is important to choose an appropriate window function (here, it is a Hanning window). By finding the fundamental frequency (f_o) value of the signal we can easily obtain the synchronization with respect to the frequency and can adapt this to the final harmonic and interharmonic analysis.

CHAPTER V

CASE STUDY PROCESSED DATA

5.1 Introduction

In order to demonstrate the proposed method with an actual shipboard power quality study, some real-time data acquired from the USCGC Healy is used. As explained in Chapter II, the Healy contains two 12-pulse converter drive systems supplied from four 7.2MW generators, as shown in Figure 2.5. The voltage was sampled at the 6.6kV bus location 1P using Ross voltage dividers and National Instruments data acquisition equipment. The measurements presented here were registered at different load conditions of a bollard (pushing against a large stationary body of ice), at a sampling frequency of 7680Hz with generator one (1G) and generator four (4G) on-line.

The analyzed waveform shown in Figure 5.1 corresponds to 12 cycles of the fundamental period of Phase-*A* Voltage at full load condition with two generators. Here, the window size was chosen to be T_w = 0.2sec, so that the fundamental frequency (f_1) is a multiple of frequency resolution f_{min} (= 5Hz). This waveform contains harmonics along with interharmonics. Difficulty in detecting the fundamental occurs if interharmonics are present in the main frequency bin of the fundamental. It has been observed that the

presence of the interharmonics in the main bins of the harmonics is not always of the same extent. Hence, a harmonic with the minimum interharmonic content in its frequency bin is identified and the fundamental of the input sampled signal is determined.

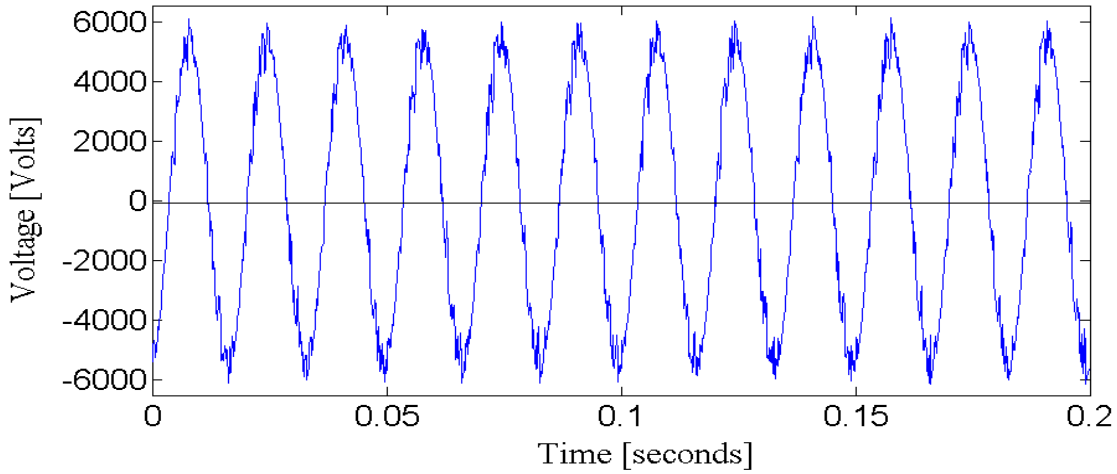

Figure 5.1 Waveform acquired from the UCGC Healy with sampling frequency (f_s) = 7680Hz.

All of these aspects are discussed in detail in this chapter by considering a test case analysis before analyzing the shipboard data in order to better understand the algorithm and proposed techniques.

5.2 Double Stage Signal Processing

To analyze the interharmonics present in the signal, the double stage interharmonic processing technique [5] has been used for this analysis; "First the fundamental frequency is detected with considerable accuracy, then harmonics are estimated and are subtracted from the original signal to get the interharmonic estimation without the influence of harmonic spectral leakage". The technique accuracy is related to

the filtering accuracy and computational burden. This technique is further described in the following two subsections.

5.2.1 Harmonic Estimation

A sampled multi-frequency signal (in the time domain) along with interharmonic frequencies is considered:

$$x(t) = \left[\sum_{m=1}^{K} A_m \sin(2\pi f_m t + \phi_m) + x^i(t) \right] \tag{5.1}$$

with sampling frequency $f_s = \frac{1}{t}$. Here, $x^i(t)$ corresponds to the interharmonic content of the signal. Expressing Equation 5.1 in the frequency domain results in the following format,

$$X[k] = \left[X^H[k] + X^I[k] \right]; \tag{5.2}$$

i.e., the signal is represented by the sum of two contributions, one that is harmonic, and the other, interharmonic.

Now, the 1st stage Hanning window is adapted to the original signal:

$$X_\omega[k] = \left[X^H[k] + X^I[k] \right] W_h[k] \tag{5.3a}$$

$$X_\omega[k] = X[k] \; W_h[k] \tag{5.3b}$$

Using the algorithm developed in Chapter IV of this thesis estimation of the fundamental frequency, $\hat{f}_1$, and hence harmonic frequencies, $\hat{f}_m$, along with the phase, $\hat{\phi}_m$, and amplitudes, $\hat{A}_m$, are determined (see the Appendix).

The estimation $\hat{f}_m$, $\hat{\phi}_m$, $\hat{A}_m$ of all the harmonic components gives:

$$\hat{x}^h(t) = \sum_{m=1}^{K} \hat{A}_m \sin(2\pi \hat{f}_m t + \hat{\phi}_m) \tag{5.4}$$

This harmonic component can be subtracted (filtered) from the original signal, as shown in Equation 5.1 to get the residual part, which consists of interharmonics:

$$\hat{X}^I[k] = X[k] - \hat{X}^H[k] \tag{5.5}$$

In the time domain, the same can be written as:

$$\hat{x}^i(t) = x(t) - \hat{x}^h(t) \tag{5.6}$$

The accuracy of the interharmonic estimation depends on the accuracy of the estimation of the harmonic frequency, $\hat{f}_m$, amplitude, $\hat{A}_m$, and phase, $\hat{\phi}_m$ of the signal to be filtered.

The error of the filtered signal is the leakage and is given by:

$$\varepsilon^H[k] = X^H[k] - \hat{X}^H[k] \tag{5.7}$$

Lower values of ε^H imply the lower values of leakage, and increased accuracy for the interharmonic analysis.

5.2.2 Interharmonic Estimation

The obtained $\hat{x}^h(t)$, in the frequency domain $\hat{X}^I[k]$, is free of harmonics, and is now considered to be the next stage signal to be analyzed. This interharmonic analysis can be conducted in the same way as the harmonic estimation.

Apply a 2nd stage Hanning window to $\hat{X}^H[k]$:

$$\hat{X}_\omega^H[k] = \hat{X}^H[k] \; W_h[k] \tag{5.8}$$

Applying the Hanning window for the second time will reduce the leakage caused by ε^H, as seen in Equation 5.7. Thus, it will increase the accuracy for further analysis. The interharmonics from Equation (5.8) can be obtained by DFT spectrum.

In actual measured signal analysis, the interharmonics generated because of numerous high power non-linear loads will be higher in number and will therefore, fall in closer frequency bins. For this case, analysis of each individual interharmonic may not be possible. A technique called IEC grouping [4] is briefly discussed in Chapter VI to overcome this problem. This will give a good estimate for the harmonic and interharmonic analysis.

Prior to the analysis of harmonic and interharmonic frequencies, using modified double stage signal processing with the signals, it is better to have knowledge of the signal processing technique with current standards. "The latest IEC standard drafts 61 000-4-7 and 61 000-4-30 contain methods of measurements and interpretation of results for harmonic and interharmonic distortion." Section 5.3 deals with the signal processing procedures, with an exception to the IEC standard draft, used for the analysis of the data to meet the standards corresponding to increased accuracy.

5.3 Recommended Signal Processing

IEC standard draft [6] signal processing recommendations are followed with the exception of using a weighted Hanning window instead of a rectangular window, to minimize the effect of the spectral leakage, and to minimize the effect of interharmonics (interpolation) on the main harmonics.

Based on the IEC standard draft, the adapted signal processing for the signal analysis to be performed is shown as follows:

- *Sampling frequency* (f_s): 7680Hz.
- *Window width* (T_W): Exactly 12 cycles of the fundamental period, T_1, corresponding to the fundamental frequency of 60Hz.
- *Window weighting*: The sampled signal is weighted with the Hanning window (HW).
- *Discrete Fourier Transform* (DFT): should be performed with 5Hz of frequency resolution.

5.4 Accuracy

With the proposed algorithm discussed in Chapter IV, the results in calculating the fundamental with the extent of desynchronization have improved the accuracy. This is shown in Figure 5.2 where the results of the proposed algorithm are compared with the standard interpolated FFT method [7] for a Hanning Window.

The algorithm resulted in much more accurate results than interpolation method. This can be explained as follows: First, desynchronized sampled signal are analyszed using signal-processing technique (Section 5.2 and Section 5.3) based on Hanning window properties. Secondly, the weighted Hanning window is used for both stages of double stage signal processing technique. As the same procedure is applied for all harmonics, including the fundamental, the error caused by negotiating the negative frequency replica is reduced in order to increase the accuracy [7].

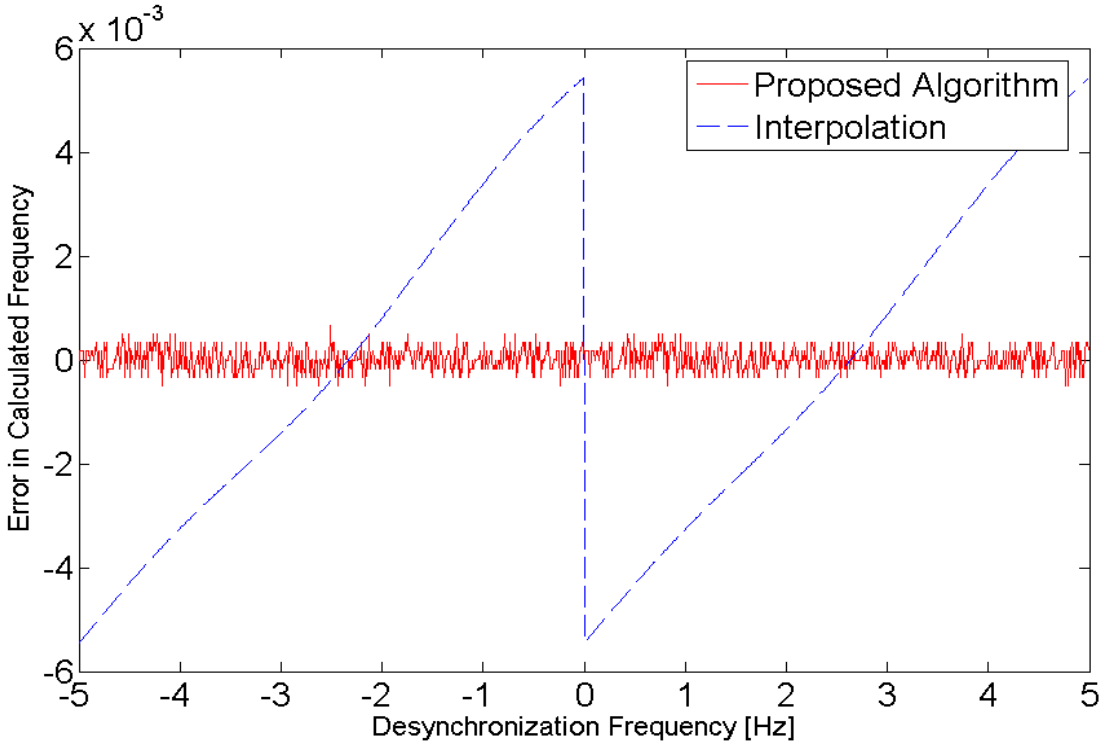

Figure 5.2 Error in calculated frequency vs. desynchronization in the fundamental frequency.

As described previously, before applying the proposed algorithm to the Healy case study measured data, the performance was analyzed using simple case studies. The following section deals with the analysis of the numerical test case signal by introducing harmonics and interharmonics into a basic fundamental signal. The signal is constructed in the view of a 6-pulse converter drive, where the 5^{th}, 7^{th}, 11^{th} and 13^{th} harmonic frequencies are dominant.

5.5 Numerical Tests

A numerical test with a simple case study (with interharmonics present outside of the main lobe of the fundamental frequency) is performed to confirm the accuracy and

robustness of the proposed technique. Harmonic tones present in this case study are as shown in Table 5.1.

Table 5.1 Case study harmonic tones

Frequency [Hz]	59.85	299.25	418.95	658.35	778.05
Amplitude [%]	100	1.2	1.6	4.6	4
Phase [Degree]	0	90	60	90	45

Here, for a sampling frequency (f_s) of 7680Hz, the value of the fundamental frequency (f_1) is deliberately kept at 59.85Hz, instead of 60Hz., i.e. f_s is not an integer multiple of f_o. So there exists incoherent sampling, or desynchronization between the actual fundamental (f_o) and the true fundamental (f_i) values of the frequency. The harmonics presented here are the 5^{th}, 7^{th}, 11^{th} and 13^{th} order of the fundamental frequency, which are dominant harmonics in a typical case of a 6-pulse cyclo-converter.

For this sampled signal, interharmonic frequencies are added, keeping their amplitudes below 1% of the value of fundamental amplitude, to cope with the practical measured signals. The interharmonic frequencies along with their amplitudes as a percentage value of fundamental amplitudes are shown in Table 5.2.

Table 5.2 Case study interharmonics

Frequency [Hz]	90	338	575	725
Amplitude [%]	0.4	0.3	0.4	0.4
Phase [Degree]	90	90	90	90

As mentioned previously this is a simple case study, i.e. frequencies of the interharmonics presented here do not fall in the main bins of the fundamental and harmonic frequencies. This kind of situation will be observed in the case of light loads, where the interharmonics will be in less in number. The waveform of this signal along with the harmonic and interharmonic distortion for a window length of T_w = 0.2sec is given in Figure 5.3.

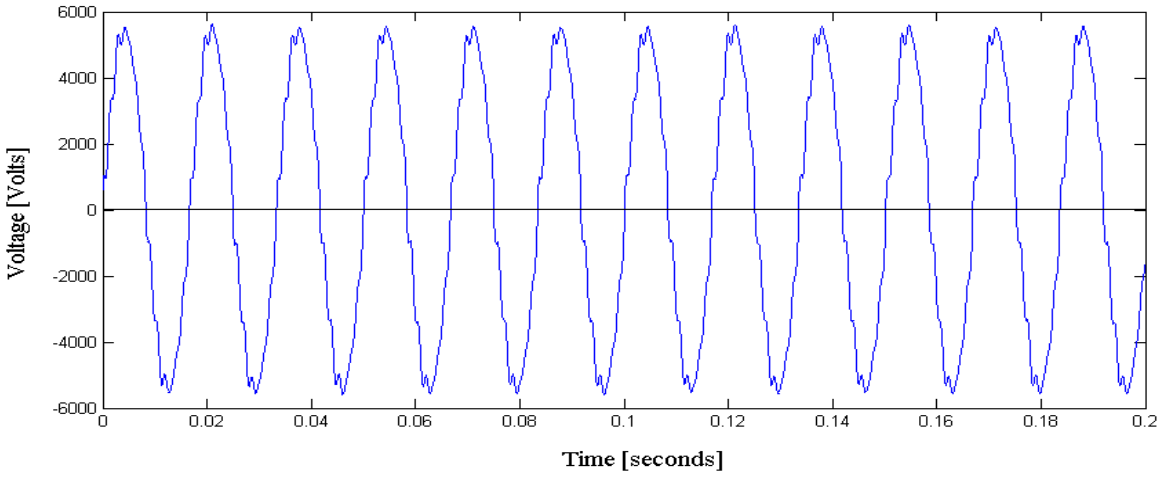

Figure 5.3 Waveform of the signal for simple case study.

Figure 5.4 shows the DFT components of the signal for the given case study, obtained by weighting the signal with a Hanning-Window (HW) of sample length of 1536 samples, equivalent to a window size of $T_w = 0.2$sec for a sampling frequency (f_s) = 7680Hz.

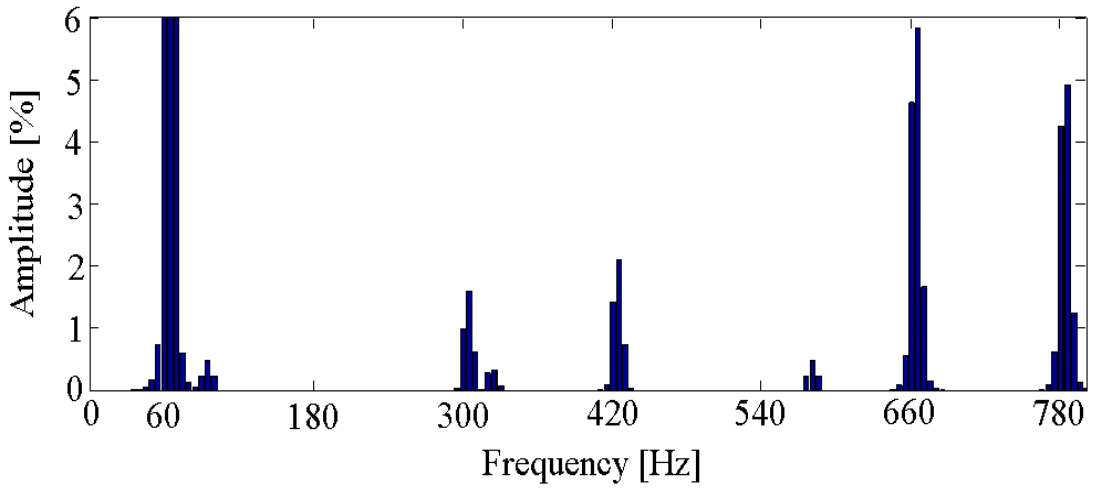

Figure 5.4 Spectral components for case study with HW.

From the algorithm explained in Chapter IV, the results (approximated to 4 decimal points) for this case study can be obtained as shown in Table 5.3.

Table 5.3 Harmonic tones from the simulation

Frequency [Hz]	59.8499	299.2498	418.9501	658.3501	778.0499
Amplitude [%]	99.9347	1.1994	1.5990	4.5979	3.9983
Phase [Degree]	0.0036	90.04771	60.0260	90.0436	45.0507

Comparing the results of Table 5.3 with the actual inserted harmonics from Table 5.1, the value of the fundamental has an error of $1.67 \otimes 10^{-4}$, which is in most cases negligible. Thus with the help of the proposed algorithm, the fundamental frequency of the sampled signal in the presence of the harmonics and interharmonics is successfully obtained with a reasonable accuracy.

After getting the value of the fundamental, we can easily obtain the corresponding values of harmonic frequencies and their amplitudes. After getting those values for the given sampled signal, subtract them from the original signal to get the residue value of the interharmonic frequencies and their amplitudes. Figure 5.5 shows the DFT components of the signal after subtracting the fundamental and harmonic content from the original signal.

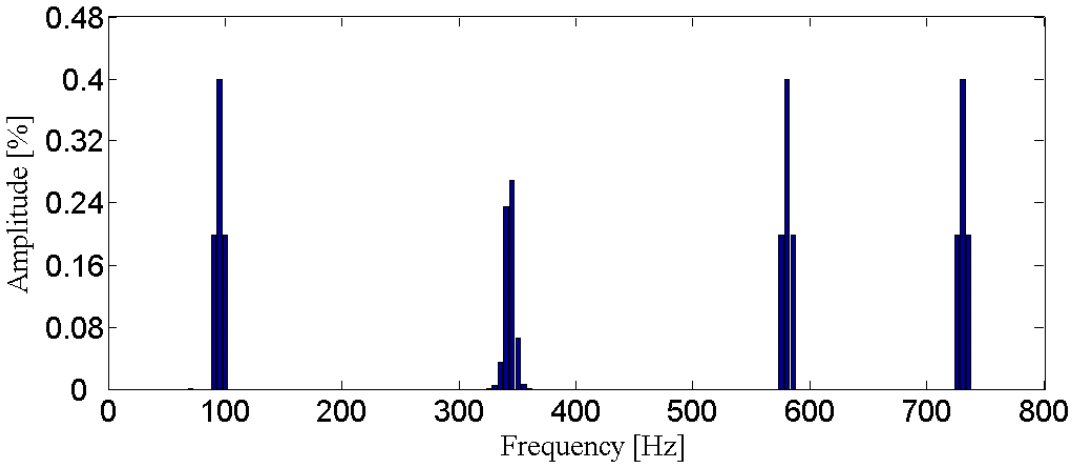

Figure 5.5 Spectral components of interharmonics for case study with HW.

Table 5.4 gives the values of corresponding interharmonic frequencies and their amplitudes after the removal of the harmonic content from the original signal.

Table 5.4 Interharmonic tones from simulation

Frequency [Hz]	90.0001	337.9976	575.0001	725.0001
Amplitude [%]	0.4003	0.3001	0.4002	0.4003
Phase [Degree]	89.8827	89.8875	89.8833	89.8832

By comparing the values of the interharmonic frequencies of Table 5.4 with the values in Table 5.2, we observe the value of the error is small and can be acceptable in the practical analysis of the measured data signals.

CHAPTER VI

APPLICATION TO HEALY SHIPBOARD SYSTEM

This chapter is concerned with the application of the proposed method to an actual shipboard power quality study, i.e. the measurements acquired from the USCGC Healy under different pulsating load conditions.

Figure 6.1 shows the Healy distribution system one-line diagram along with the National Instrument's PXI data acquisition system onboard. As the cyclo-converter drive loading increases on the system, more and more interharmonics are injected, making the measured and acquired data further distorted. The measurements presented in Figure 6.2 were 3-phase registered voltages at full load conditions of a Bollard (pushing against a large stationary body of ice), at a sampling frequency of 7680Hz with generator one (1G) and generator four (4G) on-line.

In Reference [15] the authors presented a signal processing approach, which does not require synchronization to analyze harmonics and interharmonics. For this kind of analysis, the main goal is to find the fundamental frequency as accurately as possible. Increased accuracy of the interharmonic estimation in the frequency domain depends mainly on the accuracy of the fundamental. The presence of the interharmonics in the main bins of the fundamental and the harmonics can influence the accurate estimation of their respective frequency values.

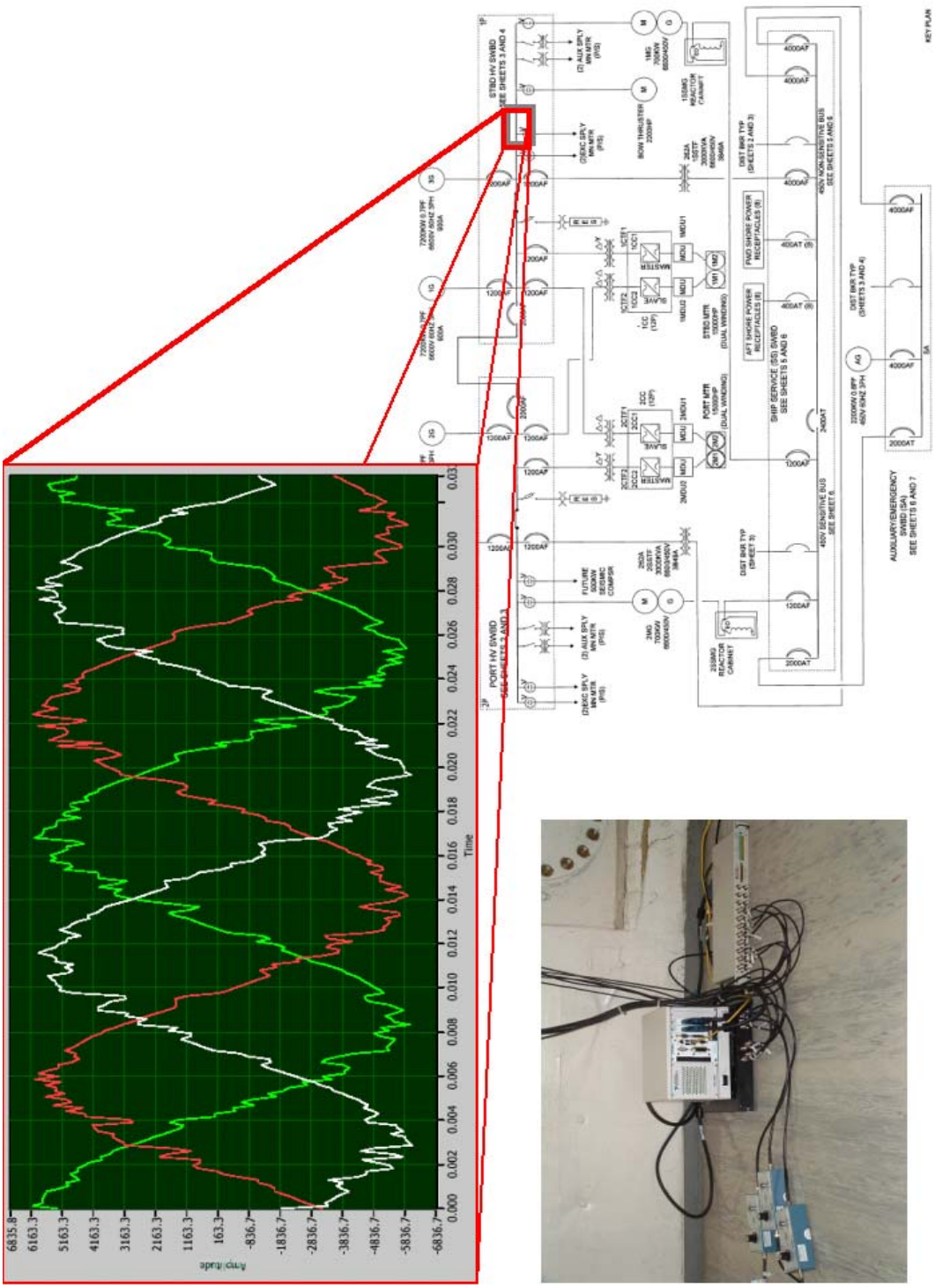

Figure 6.1 Healy one-line diagram from Figure 2.5 along with the PXI data acquisition system onboard.

Nevertheless, the error caused seems to give an acceptable accuracy reduction as shown in Chapter V with the case study data (Table 5.1 and Table 5.3). A similar process of analysis can be extended for the online shipboard acquired data.

For the measurement data shown in Figure 6.2, the signal spectrum is first evaluated using a DFT. Figure 6.3 shows the amplitude spectrum of the all the harmonic content (taken up to the 55th harmonic of the fundamental frequency) for Phase-A voltage in percentage of the fundamental amplitude. By performing the analysis using the proposed algorithm in Chapter IV, the fundamental of this waveform is found to be 60.1184Hz and the amplitude is 5468.4 Volts.

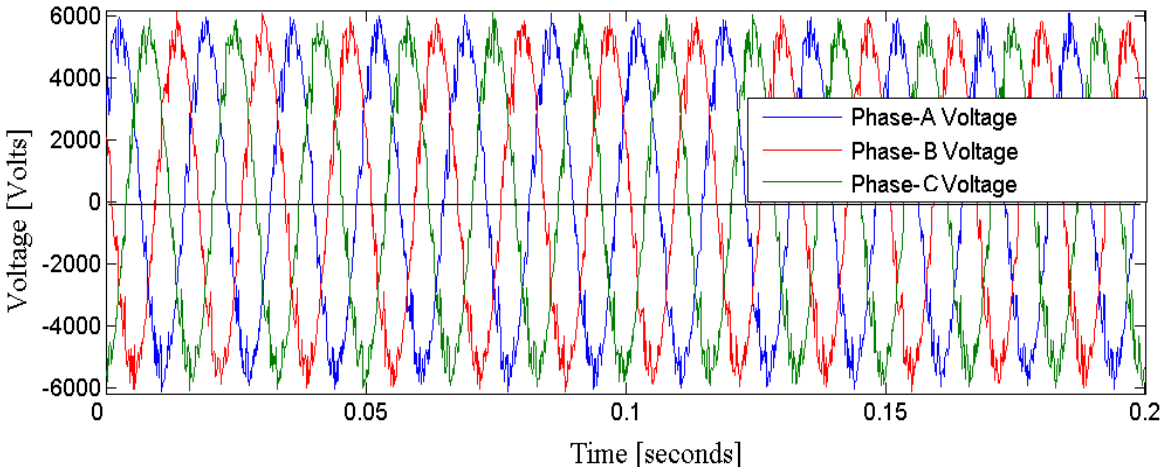

Figure 6.2 Wave form acquired from the Healy with sampling frequency (f_s) = 7680Hz.

In this kind of spectrum analysis, finding the details of the individual harmonics is a difficult task. To reduce the calculation burden, in the first stage, the actual frequencies, amplitudes, and phase angles of harmonics of the order $12k \pm 1$, i.e. 11th, 13th, 23rd and 25th etc. (which are dominant in a 12-pulse cyclo-converter), including the fundamental,

are estimated using the techniques of Section 5.2 and Section 5.4 in the frequency domain; the estimated components are then filtered away from the original signal.

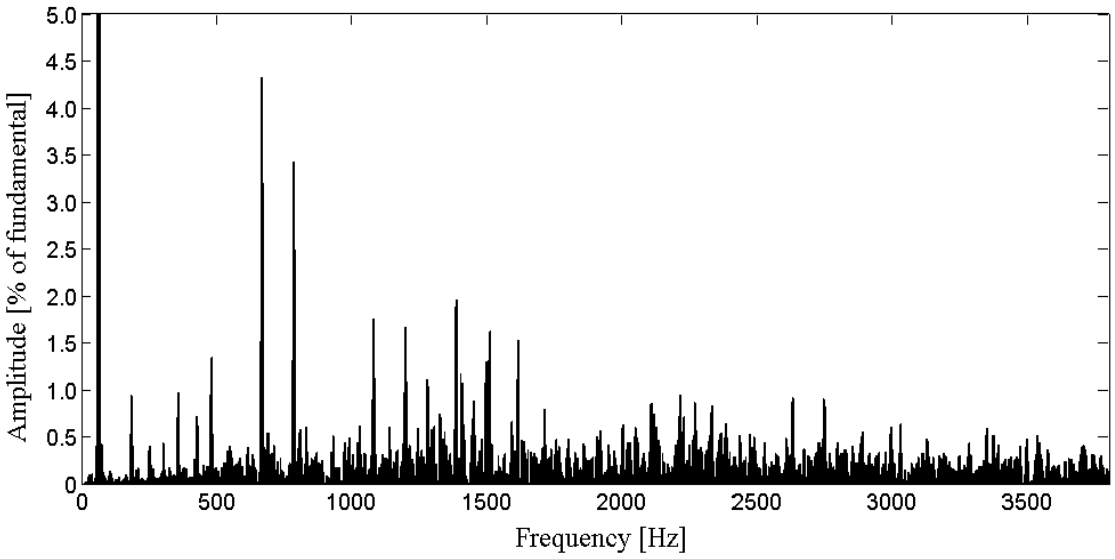

Figure 6.3 Complete DFT harmonic spectrum for Healy Data.

Table 6.1 gives the corresponding numerical values of the frequencies, amplitudes, and phase angles for the estimated harmonics of Phase-A measured voltage data. Notice that the harmonic amplitudes corresponding to the 11^{th} and 13^{th} harmonics are dominant, which is expected for a 12-pulse converter. From these values in Table 6.1, the signal waveform can be constructed by using Equation 5.4.

Figure 6.4 gives the constructed signal, for Phase-A voltage measurement, from the 1^{st} stage harmonic estimation including the fundamental in the time domain. This estimation can also be applied to the Phase-B and Phase-C voltages yielding a complete analysis of the acquired data signal.

Table 6.1 Harmonic tones for Healy measured data

Frequency [Hz]	Voltage [Volts]	Phase angle [deg]
60.1184	5468.4	396.25
300.592	24.9	164.52
420.8288	43.8	106.69
661.3024	248.4	126.38
781.5392	195.8	111.25
1022.0128	35.1	303.61
1142.2496	33.7	417.42
1382.7232	123.9	159.47
1502.96	96.2	143.48
1743.4336	27.7	39.54
1863.6704	27.3	232.96
2104.144	55.4	97.24
2224.3808	42.2	340.04
2464.8544	30.2	49.41
2585.0912	29.1	305.42
2825.5648	23.9	117.4
2945.8016	20.5	274
3186.2752	20.9	81.68
3306.512	12.5	151.98

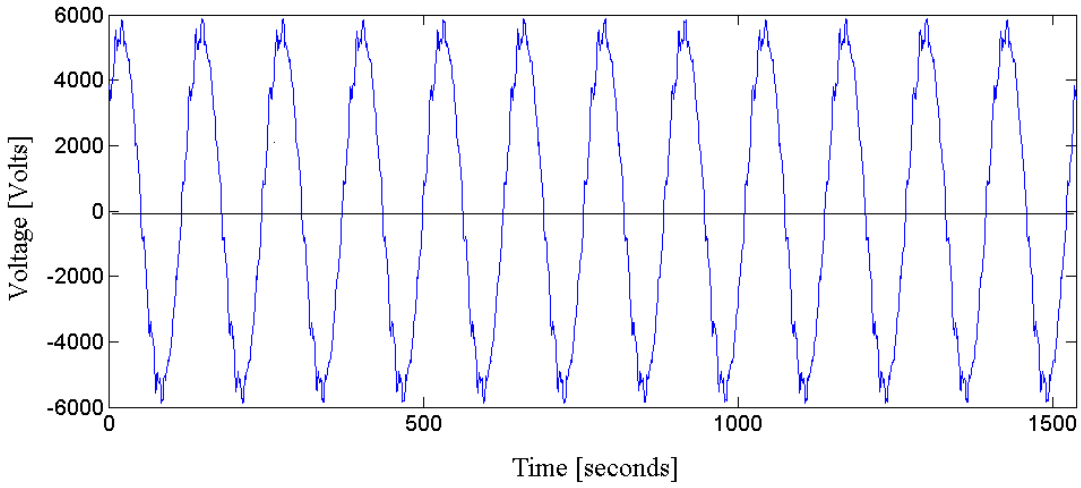

Figure 6.4 Waveform constructed from the estimated harmonics including the fundamental.

After estimating the first stage harmonic frequencies, amplitudes, and phases in the time domain, they can then be filtered away using Equation 5.6.

Figure 6.5 shows the amplitude spectrum of the interharmonics after filtering the main harmonic content, in terms of a percentage of the fundamental frequency amplitude. It is noticeable from the interharmonic spectrum, unlike the main harmonics, finding the detail of each individual interharmonic is a difficult and time-consuming task.

A significant simplification can be obtained [4], by reducing the detailed knowledge about the interharmonics in terms of frequency localization and single component amplitude evaluation. Introducing the technique of harmonic and interharmonic grouping can do this.

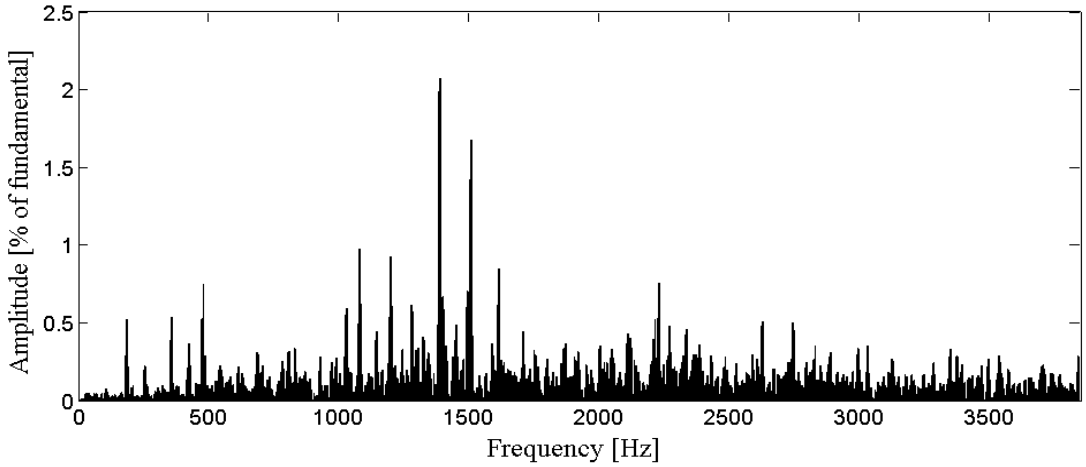

Figure 6.5 Spectrum of interharmonic frequencies for Healy.

Figure 6.6 shows the results of the IEC grouping technique for the spectral components having both harmonic (5^{th} and 6^{th} harmonic sub-group) and interharmonic (5.5 interharmonic sub-group) components.

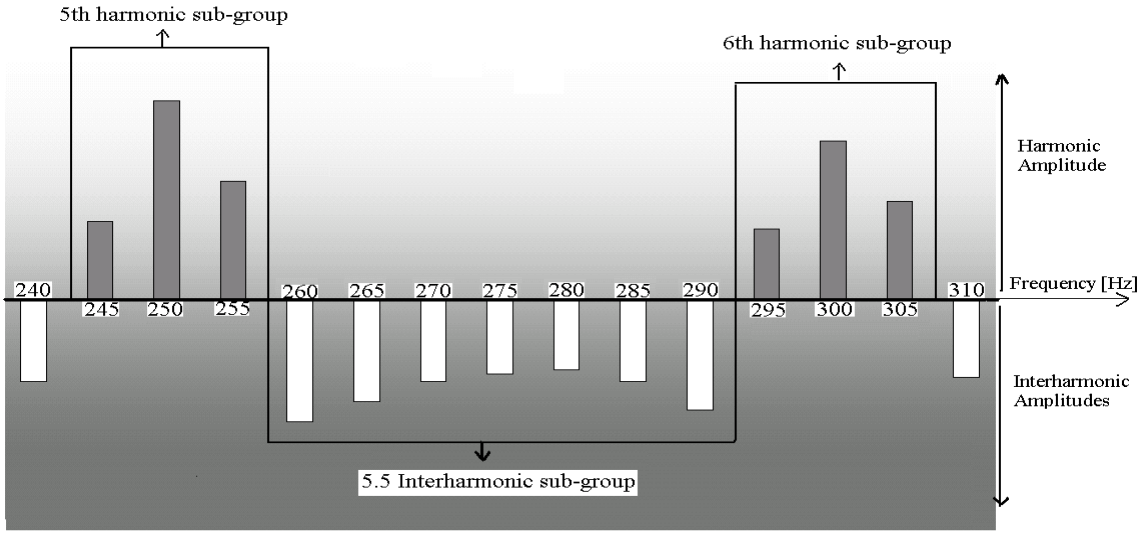

Figure 6.6 IEC grouping of spectral components for 5^{th} and 6^{th} harmonic group ↑, and for 5.5 interharmonic group ↓.

The definition of the different harmonic groups for a 60Hz system is given as follows:

Harmonic subgroup (HG) of amplitude $C_{n-200-ms}$: This harmonic group is defined as,

$$C^2_{n-200-ms} = \sum_{k=-1}^{1} C^2_{12n+k} \,, \tag{6.1}$$

where $C_{n-200-ms}$ is *RMS* value of the n^{th} order harmonic group on a widow size of 200 ms.

Interharmonic subgroup (IG) of amplitude $C_{n+0.5-200-ms}$: This interharmonic group is defined as,

$$C^2_{n+0.5-200-ms} = \sum_{k=2}^{10} C^2_{12n+k} \,, \tag{6.2}$$

where $C_{n+0.5-200-ms}$ is the *RMS* value of the $(n+0.5)^{th}$ order interharmonic group on a widow size of 200 ms.

Harmonics and interharmonics are calculated for the Healy analysis measured data, using the IEC Harmonic Grouping (HG) technique with HW [4]. Figure 6.7 shows the detailed values of each of the harmonic and interharmonic amplitudes.

It is worth noting that the IEC *Harmonic Grouping* technique gives a better approximation of the interharmonics. Using the proposed algorithm, the location of a peak interharmonic can be located with considerable accuracy. Suppose, in this particular analysis, that by looking at the plots in Figure 6.5 and Figure 6.7 it can be seen that the peak value of the interharmonic is located around 25^{th} harmonic frequency.

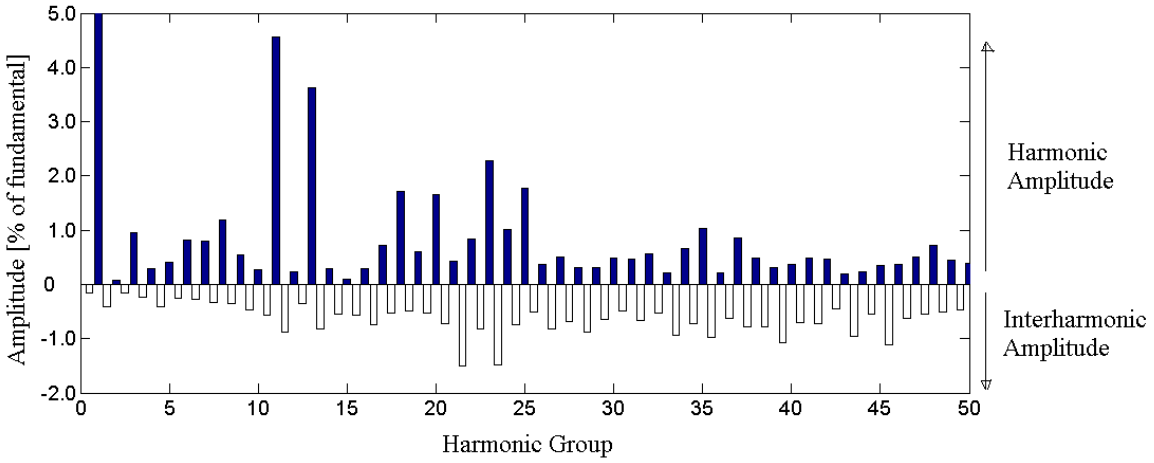

Figure 6.7 IEC grouping of spectral components for Healy Data, harmonics ↑, and interharmonics ↓.

With the proposed algorithm the exact frequency, amplitude, and the phase angle corresponding to that particular interharmonic can be found. Table 6.2 gives the corresponding values found from the algorithm.

Table 6.2 Values corresponding interharmonic frequency of maximum amplitude.

Frequency [Hz]	Amplitude [Volts]	Phase angle [deg]
1383.7884	111.4	200.43

Figure 6.8 gives the comparison of the harmonic amplitude values obtained both from the Algorithm and the IEC Harmonic Grouping technique, and Table 6.3 gives the corresponding numerical values. It can be noticed that there is a very small variation in the value of the amplitudes of the harmonics, but with the proposed method it is also possible to find the frequency and phase information with considerable accuracy.

.

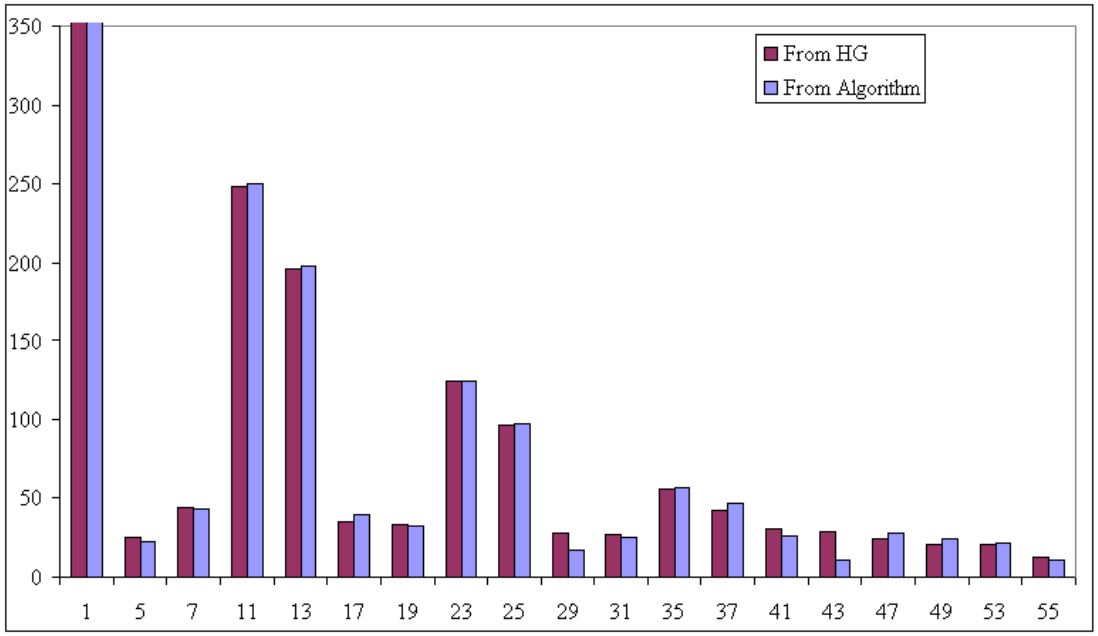

Figure 6.8 Comparison of harmonic spectral components for Healy Data.

Figure 6.9 shows the comparison of interharmonic tones as a percentage of the fundamental by using Harmonic Grouping technique.

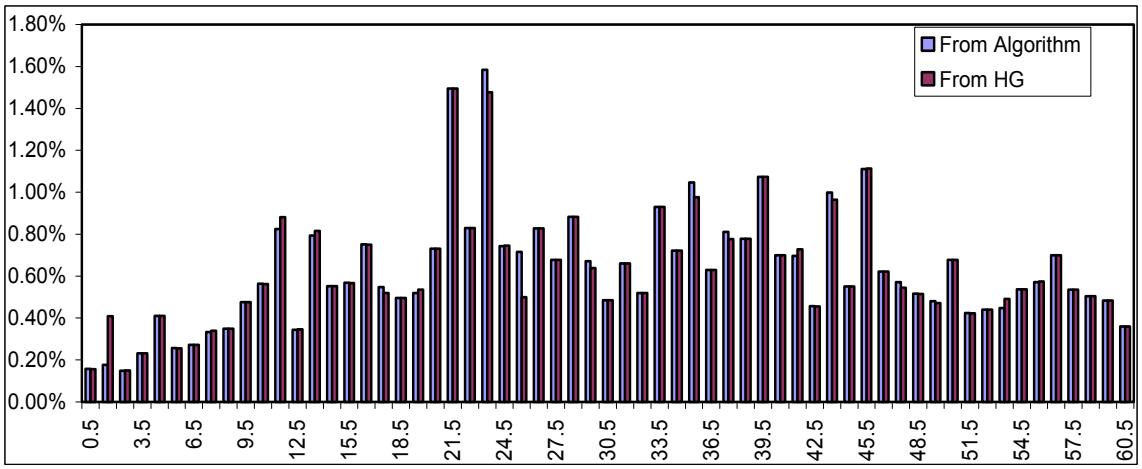

Figure 6.9 Comparison of interharmonic spectral components for Healy Data.

Table 6.3 Comparison of harmonic tones for Healy measured data.

.

Frequency Harmonic	From Algorithm	From Harmonic Grouping
Fundamental	5468.4	5473.42
5th	24.9	22.05
7th	43.8	43.31
11th	248.4	249.73
13th	195.8	198.09
17th	35.1	39.23
19th	33.7	32.73
23rd	123.9	124.28
25th	96.2	97.01
29th	27.7	17.46
31st	27.3	25.11
35th	55.4	56.41
37th	42.2	46.37
41st	30.2	26.4
43rd	29.1	10.69
47th	23.9	27.73
49th	20.5	24.43
53rd	20.9	22.01
55th	12.5	10.36

Now, consider a portion of the Healy sampled data with a difference in the fundamental frequency that is very large compared with the 60Hz-sampled system, where the fundamental frequency of the sampled data is 58.76Hz. Using the Harmonic Grouping technique, the spectrum can only be calculated by considering the fundamental as 60Hz, which will give an incorrect estimation of higher order harmonics as the shift in frequency bin (to be grouped to calculate the harmonics amplitudes) position will increase with the harmonic order. This can be explained as follows:

From Equation 6.1, the values of the harmonics are given by

$$C^2_{n-200-ms} = \sum_{k=-1}^{1} C^2_{12n+k} \quad , \tag{6.1}$$

for n = 11, i.e. for 11th harmonic order, the corresponding grouping is performed by calculating the values of C_{131}, C_{132} and C_{133}, which are the frequency bins of 655Hz, 660Hz and 665Hz respectively. With the fundamental frequency of 58.76Hz, we get the frequency of the 11th order harmonic as 646.36Hz. This means that with the Harmonic Grouping Technique, the frequency bins (C_{129}, C_{130} and C_{131}) that contain the actual 11th order harmonic are not taken into consideration at all, resulting in an incorrect value in the final analysis estimation, which is obvious from Figure 6.10.

Reference [4] states that for analysis using Harmonic Grouping "an uncertainty of (desynchronization) $\Delta f = \pm 10\,\text{mHz}$ is allowed, and such a level of uncertainty can be assumed on the estimation value of T_w that one could try to adapt by also considering the finite frequency resolution of the sampling clock". Also, as the uncertainty

(Δf) increases, the grouping technique makes the calculation of harmonic amplitudes less accurate.

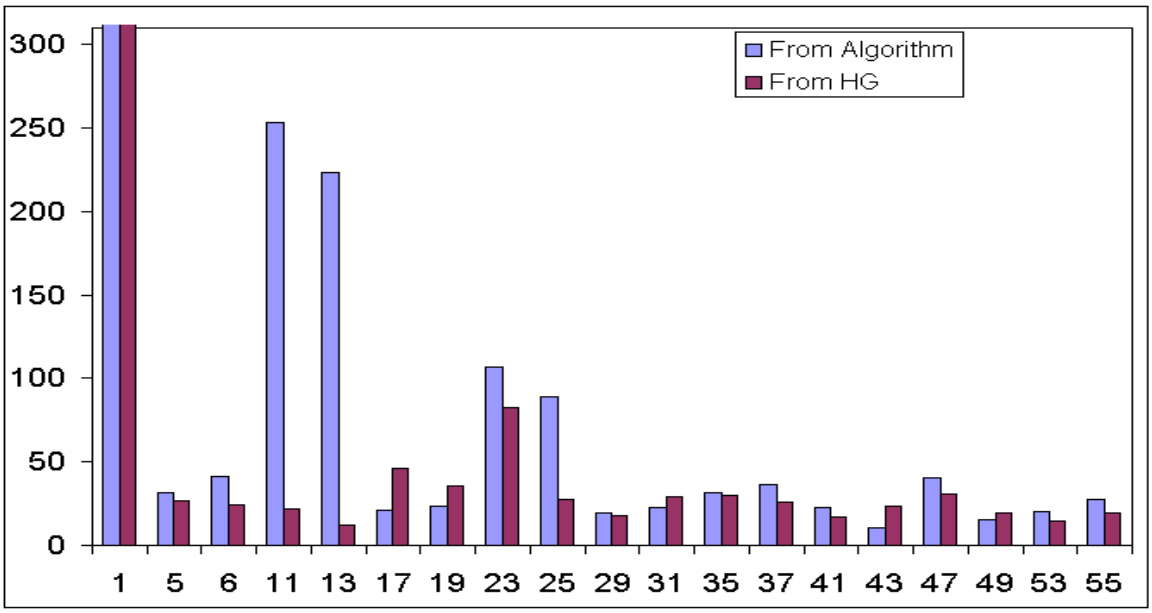

Figure 6.10 Harmonic spectral components for Healy Data (with fundamental frequency = 58.76Hz).

The proposed algorithm discussed in this thesis will give better results in this kind of situation in estimating the values of the higher harmonic amplitudes, as compared with the Harmonic Grouping technique. Taking real data from USCGC Healy, the results are validated.

CHAPTER VII

CONCLUSION

A novel approach to finding the fundamental of a desynchronized sampled signal is proposed. Using the proposed algorithm, the error caused by negotiating the negative frequency replica, in the interpolation FFT method, is reduced in order to increase the accuracy. The error in resultant fundamental frequency, calculated from the proposed algorithm with the desynchronization, is compared with the interpolation method, and demonstrates improved results.

The technique is then extended to find the interharmonics based on the double stage signal processing technique. The results are validated with numerical tests by considering case study harmonic and interharmonic tones. Then the technique is further applied to analyze data recorded during an actual shipboard power quality study, i.e. the measurements acquired from the UCSGC Healy under different pulsating load conditions.

This thesis presents the difficulties in estimating the frequency values in spectrum analysis of the acquired measured data from the real system, and the problem caused by using the IEC grouping technique for cases where the fundamental frequency is substantially desynchronized with the sampling system. A better method of estimating the

harmonic and interharmonic estimation is presented using a modified grouping technique, by first estimating major harmonic content of the data signal, and then estimating the remaining spectrum with a grouping technique. Although finding all possible interharmonics in a signal is difficult with this technique or any technique, it is possible to calculate the parameters of a particular interharmonic with good accuracy, in a given range of frequency.

REFERENCES

[1] M. Hernes and B. Gustavsen, "Simulation of shaft vibrations due to interaction between turbine-generator train and power electronic converters at the visund oil platform," in *Proceedings of Power Conversion Conference*, vol. 3, Osaka, Japan April 2002, pp. 1381-1386.

[2] R. Carbone, D. Mennitti, R. E. Morrison, A. Testa, "Harmonic and Interharmonic Distortion Modeling in Multiconverter Systems," *IEEE Trans. Power Delivery*, Vol.10, NO. 3, pp. 1685-1692, July 1995.

[3] A. Ferrero, R. Ottobani, "A Low-Cast Frequency Multiplier for Synchronous Sampling of Periodic Signals," *IEEE Trans. Instrumentation and Measurement*, Vol.41, NO. 2, pp. 203-207, 1992.

[4] Daniele Gallo, Roberto Langella, Alfredo Testa, "On the Processing of Harmonics and Interharmonics in Electrical Power Systems," *IEEE Trans. Power Delivery*, pp. 1581-1586, 2000.

[5] Daniele Gallo, Roberto Langella, Alfredo Testa, "Double Stage Harmonic and Interharmonic Processing Technique," *Proceedings of the IEEE*, pp 1141-46, 2002.

[6] IEC standard draft, CEI 1000-4-30, 77A WG9 TF1.

[7] V. K. Jain, W. L. Collins, D. C. Davis, "High-Accuracy Analog Measurement Via Interpolated FFT*," IEEE Trans. Instrument and Measurement*, Vol. 28, No. 2, pp. 114-115, June 1979.

[8] Alf Kåre Ådnanes, "Maritime Electrical Installations and Diesel Electric Propolsions," *ABB*, April 2003.

[9] Fredric J. Harris, "On the Use of Windows for Harmonic Analysis with the Discrete Fourier Transform," *Proceedings of the IEEE*, pp 51-63, Vol. 66, No.1, January 1978.

[10] Sophocles J. Orfanidis, "Introduction to Signal Processing," Prentice-Hall ISBN 0-13-209172-0.

[11] R. F. Chu and J.J. Burns. "Impact of Cyclo-converter Harmonics," *IEEE Transactions on Industry Applications*, Vol. 25, No. 3, May/June 1989, pp. 427-435.

[12] Bishop, G.N., N.A Shelley and M.J.S.Edmonds, "Electric propulsion of surface fighting ships," *Proceedings of Eleventh Ship Control Systems Symposium*, pp. 157-171,vol.2, April 1997

[13] Fracchia M. and Sciutto G., "Cycloconverter Drives for Ship Propulsion," *Proceedings of Power Electronics*, Electrical Drives, Advanced Electrical Motors, Symposium, pp. 255-260 vol. 1, 1994

[14] B. R. Pelly, "Thyristor Phase Controlled Converters and Cyclo-converters," Wiley, New York, 1971.

[15] Daniele Gallo, Roberto Langella, Alfredo Testa, "Desynchronized Processing Technique for Harmonic and Interharmonic Analysis," *IEEE Transactions on Power Delivery*, pp. 993-1001, Vol. 19, No. 13, July 2004.

[16] Anil K.Kondabathini, Herbert L. Ginn and Marshall Molen, "Accurate method to Measure Harmonic and Interharmonics in Shipboard Power Quality Analysis," *2005 Electric Ship Technologies Symposium*, pp.255-260, July 2005.

APPENDIX

ESTIMATION OF AMPLITUDE, AND PHASE ANGLE OF THE HARMONICS

In the presence of desynchronization between tone and sampling frequency, none of the DFT components matches the actual frequency as shown in Figure A.

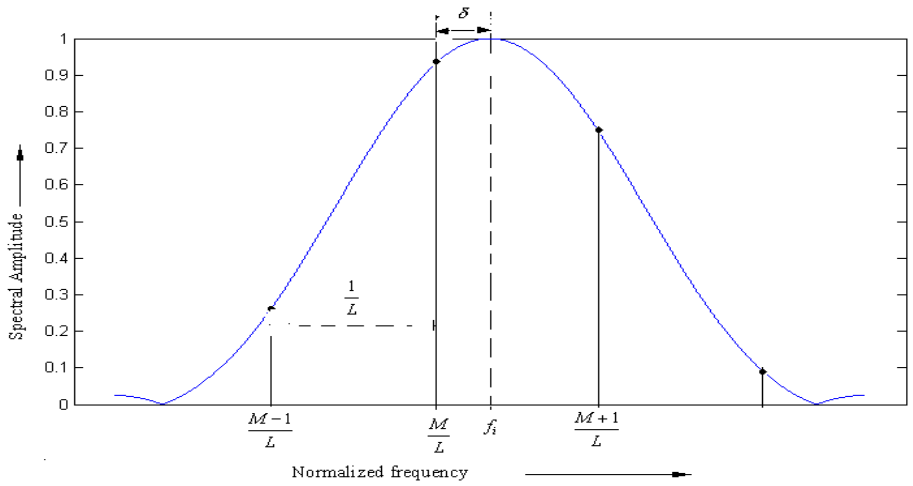

Figure A.1 Normalized frequency spectrum of a given signal.

Here, the proposed algorithm in Chapter IV determines the actual tone frequency. The actual amplitude can be evaluated from the DFT components nearest to the actual tone frequency by means of the following relation [5].

$$A_m = \pi \left| S(M) \right| \frac{\delta_m \left(1 - {\delta_m}^2\right)}{\sin(\pi \delta_m)}, \tag{A.1}$$

where $S(M)$ is the DFT component nearest to the actual harmonic frequency and δ is the amount of desynchronization between the harmonic DFT component and the actual harmonic frequency.

Similarly the phase angle can be evaluated as:

$$\phi_m = \frac{\pi}{2} + \angle S(M) - M \pi \delta_m . \tag{A.2}$$